National Library of Canada

Acquisitions and Bibliographic Services Branch

395 Wellington Street
Ottawa, Ontario
K1A 0N4

Bibliothèque nationale du Canada

Direction des acquisitions et des services bibliographiques

395, rue Wellington
Ottawa (Ontario)
K1A 0N4

Your file Votre référence

Our file Notre référence

NOTICE

The quality of this microform is heavily dependent upon the quality of the original thesis submitted for microfilming. Every effort has been made to ensure the highest quality of reproduction possible.

If pages are missing, contact the university which granted the degree.

Some pages may have indistinct print especially if the original pages were typed with a poor typewriter ribbon or if the university sent us an inferior photocopy.

Reproduction in full or in part of this microform is governed by the Canadian Copyright Act, R.S.C. 1970, c. C-30, and subsequent amendments.

AVIS

La qualité de cette microforme dépend grandement de la qualité de la thèse soumise au microfilmage. Nous avons tout fait pour assurer une qualité supérieure de reproduction.

S'il manque des pages, veuillez communiquer avec l'université qui a conféré le grade.

La qualité d'impression de certaines pages peut laisser à désirer, surtout si les pages originales ont été dactylographiées à l'aide d'un ruban usé ou si l'université nous a fait parvenir une photocopie de qualité inférieure.

La reproduction, même partielle, de cette microforme est soumise à la Loi canadienne sur le droit d'auteur, SRC 1970, c. C-30, et ses amendements subséquents.

Canada

Effect of Laser Phase Noise on Multi-Channel Photonic Networks

By

Mustapha Aissaoui, Dipl. of Eng.

A thesis submitted to the
School of Graduate Studies and Research,
University of Ottawa,
in partial fulfillment of the requirements
for the degree of
Master of Applied Science (Electrical Engineering)

Ottawa-Carleton Institute for Electrical Engineering
Department of Electrical Engineering
Faculty of Engineering
University of Ottawa

ISBN 0-315-82590-1

Canada

UNIVERSITÉ D'OTTAWA
UNIVERSITY OF OTTAWA

Abstract

This thesis presents an investigation of the issues related to the phenomenon of laser phase noise in multi-channel coherent photonic networks. A theoretical analysis is carried out to predict the performance of two kinds of photonic networks, the distribution network and the multiple-access network, in the presence of laser phase noise. Two optical modulation schemes have been compared and the limitations set on laser linewidths are derived. The potential number of network users in each case has been discussed. It has been shown that on the average optical intensity modulation performs better than optical phase modulation. It has also been shown that the SCM/CD networks, using semiconductor lasers, are competitive with other multi-channel approaches above a certain range of the bit-rate per channel. Finally, a discussion on the diverse techniques to reduce the impact of phase noise on coherent photonic networks is provided.

Acknowledgements

Throughout the realization of this thesis, I have had the opportunity to work with and learn from a number of people whom I would like to acknowledge.

I wish to express my sincere gratitude to Dr. Willem Steenaart, my academic supervisor, for his scientific guidance and moral support since the beginning of this program.

I am also indebted to Dr. Peter Galko, my thesis co-supervisor, from whom I have learned many aspects of digital communications. His help and advice is greatly appreciated.

I would like to thank Dr. Mohsen Kavehrad, who welcomed me to the lightwave communications research group, and with whom I have had fruitful discussions.

Dr. Emil Savov has provided me with all the necessary explanations and details from his Ph.D thesis. I am very grateful to him.

Many thanks to all professors, colleagues, friends and support staff, at the Department of Electrical Engineering, University of Ottawa, for the good academic atmosphere.

I would like to express my sincere thanks to my parents in Algiers and my sister in Montreal for their moral support and encouragements during the course of this program.

This research was supported by a joint scholarship from CIDA and the Ministry of Universities of Algeria.

Contents

List of Figures

List of Tables

List of Symbols and Abbreviations

N	Number of channels in the distribution network.
M	Number of users in the multiple-access network.
R_b	Bit-rate per channel.
B	Receiver bandwidth for negligible laser linewidth.
Δf	Channel spacing.
R	Photodiode responsivity (A/W).
$\Delta\nu$	Full width at half maximum (FWHM) laser linewidth.
$P_{LO}(t)$	Local laser oscillator power.
f_{LO}	Local laser oscillation frequency.
$P_s(t)$	Received signal power.
f_s	Optical carrier frequency.
$\Phi(t)$	Modulated optical carrier phase.
$\theta(t)$	Phase noise.
AM	Amplitude modulation.
OPM	Optical phase modulation.
OIM	Optical intensity modulation.
β	Phase modulation index in OPM.
m_{el}	Effective AM index in OIM.
α	External modulator bias coefficient.
CNR	Carrier-to-noise ratio.

Chapter 1

Introduction

1.1 Motivation

The amount of information that is exchanged daily has been dramatically increasing so that conventional communication systems have barely been able to meet the new challenges, posed by the high data rates. The need for increased transmission capacities has led to a major research effort on optical fiber communication systems. By offering an available bandwidth of 20,000 GHz, a low signal attenuation and immunity to interference, the optical fiber makes an attractive medium for high-speed communication applications. However, because of electronic device limitations, the most advanced of today's systems still access no more than 0.1% of the available fiber bandwidth [1].

Most of the fiber-optic networks that have been so far implemented rely on direct detection receivers, where a photodetector converts the incoming optical pulses into an electrical signal. In coherent optical detection, a local oscillator wave is combined with the carrier wave, and yields a composite intermediate frequency (IF) signal that is detected by the photodiode.

Basically, coherent detection offers the following important advantages over direct detection: improved receiver sensitivity, greatly enhanced frequency selectivity, conveniently tunable optical receivers and the possibility of using alternative modulation formats to the direct intensity modulation of semiconductor laser diodes (e.g., angle mod-

ulation) [2]. Such advantages have been successfully demonstrated in many laboratory experiments of coherent optical fiber systems and networks [1]. More research has to be conducted before such networks can become commercially viable. One of the major problems in coherent communications is that of laser phase noise.

For practical coherent communication networks, it is essential to provide small size and low power consumption lasers. Semiconductor laser diodes, featuring long lifetime and high efficiency, fall in this category but suffer a large spectral linewidth and thus are not particularly coherent. This can deteriorate the performance of coherent receivers; furthermore, the effect of laser phase noise on the receiver performance will depend on the employed bit-rate and the modulation/demodulation techniques.

In this work, the impact of laser phase noise on multichannel coherent photonic networks is analyzed. We consider two kinds of networks, distribution networks where the information flow is mainly from one source to many destinations, and multiple-access networks where the flow of information is generally equal in all directions. The performance of two optical modulation schemes has been investigated in the presence of laser phase noise and the limitations on laser linewidth, that should be considered in the design of such networks, have been obtained. Some solutions to overcome the laser phase noise effect are also reviewed; a description of the phase noise cancellation techniques proposed in the literature is presented along with a discussion on their efficiency and the complexity of their implementation.

1.2 Contribution

The following is a summary of our contributions which are detailed in Chapter 3 of this thesis:

1. A theoretical investigation of the effect of laser phase noise on multi-channel photonic networks using both Subcarrier-Multiplexing and Coherent Detection (SCM/CD systems). An approximation was used to model the effect of laser phase noise, taking into account the other sources of noise, namely shot noise, thermal noise and intermodulation

distortion (IMD).

2. An optimization of the modulation/demodulation parameters for a maximum receiver sensitivity that can be achieved for any value of the laser linewidth was performed. This is followed by a comparison of the performance of SCM/CD networks for two optical modulation schemes: Optical Phase Modulation (OPM) and external Optical Intensity Modulation (OIM) in the presence of the laser phase noise. The investigation suggests the maximum permissible laser linewidths that are required with both modulation schemes to maintain a good performance of the multi-channel photonic networks. The analysis and the results are presented in Sections 3.3 and 3.4.

3. A discussion on the potential number of network users and the limitations set on it by the laser phase noise is provided in Section 3.5. Part of our results were reported in [3].

1.3 Outline of the Thesis

In Chapter 2, the concept of subcarrier-multiplexed photonic networks using coherent detection (SCM/CD networks) is introduced. The different systems architectures are presented and two kinds of modulation of the optical carrier are discussed. Following this, an outline of the problems associated with such networks is given with an emphasis on the major problem of laser phase noise.

Chapter 3 presents an investigation of the impact of the laser phase noise on the performance of multi-channel SCM/CD networks. Two kinds of networks are considered and a comparison of two optical modulation methods is carried out.

In Chapter 4, the different solutions that can be implemented to reduce the impact of the laser phase noise on SCM/CD networks are discussed and some phase-noise cancellation techniques are described.

Chapter 5 summarizes the results of the thesis and gives suggestions for further research in this field.

Chapter 2

Multi-Channel SCM/CD Networks

2.1 The Concept of SCM/CD Networks

Many alternatives have been developed for photonic networks, such as Time-Division Multiplexing (TDM), Wavelength/Frequency Division Multiplexing (WDM/FDM), Space Switching (SS) and more recently Subcarrier Multiplexing (SCM). Each approach has its attractive features and its limitations. Recently there has been much interest in microwave subcarrier multiplexing justified mainly by the fact that such an approach allows the use of the full range of existing electronic techniques, including analog and digital modulation, as well as microwave and baseband signalling [4]. Furthermore, SCM systems provide a mean to transmit several channels, with various modulation formats, using the same laser, fiber link and detector. Making use of electro-optic components and readily available microwave technology, SCM systems offer a simple way to take advantage of the full bandwidth capability of single-mode fibers.

The subcarrier multiplexing approach can be used jointly with either direct detection (SCM/DD systems) or coherent detection (SCM/CD systems). The term "coherent" used throughout this paper refers to the "spatial" coherence of the optical carrier, of which we take advantage in the mixing process on the surface of the photodiode. It does not necessarily mean, in contrast to the terminology of conventional communications theory, that the local optical oscillator is phase-locked to the incoming optical signal.

The SCM/DD approach carries the limitations inherent to the direct detection process and its technological requirements when it comes to transmit a large number of channels are very demanding. We can cite the need for wide-band lasers, photodiodes and electronic devices [5].

The idea behind the SCM/CD approach is to combine the advantages of both subcarrier multiplexing and coherent detection. We have listed the main advantages of coherent detection over direct detection in Section 1.1. On the other hand, SCM/CD systems are much more complex and suffer from the difficulties associated with coherent detection. We will be addressing this matter in Section 2.2.

Our work will emphasize on SCM/CD systems. The following sections will introduce the concept of SCM/CD networks; two kinds of networks, distribution networks and multiple-access networks, will be presented.

2.1.1 The SCM/CD Distribution Network

The architecture of an N-channel SCM/CD distribution network is illustrated in Fig. 2.1; N radio-frequency (RF) subcarriers are summed with a microwave power combiner and the resulting composite signal is used to modulate an optical carrier by means of an external electro-optic modulator. The RF subcarriers may be modulated by either analog or digital signals, a fact which makes it possible for the SCM system to accommodate both analog and digital modulations. Thus it can handle voice data, video, digital audio, high definition video and in general any combination of services. Because the composite signal, i.e., the sum of the N modulated subcarriers, is an RF waveform, the optical modulation is necessarily analog.

An important advantage of coherent SCM systems is that many information channels can be transmitted on one optical carrier, whereas in other multi-channel approaches, a separate laser per channel is required.

At the receiver end, the incoming optical wave is combined with the more powerful wave from a local oscillator. The combined wave illuminates a photodetector, the output current of which is proportional to the local oscillator amplitude. A low-noise amplifier

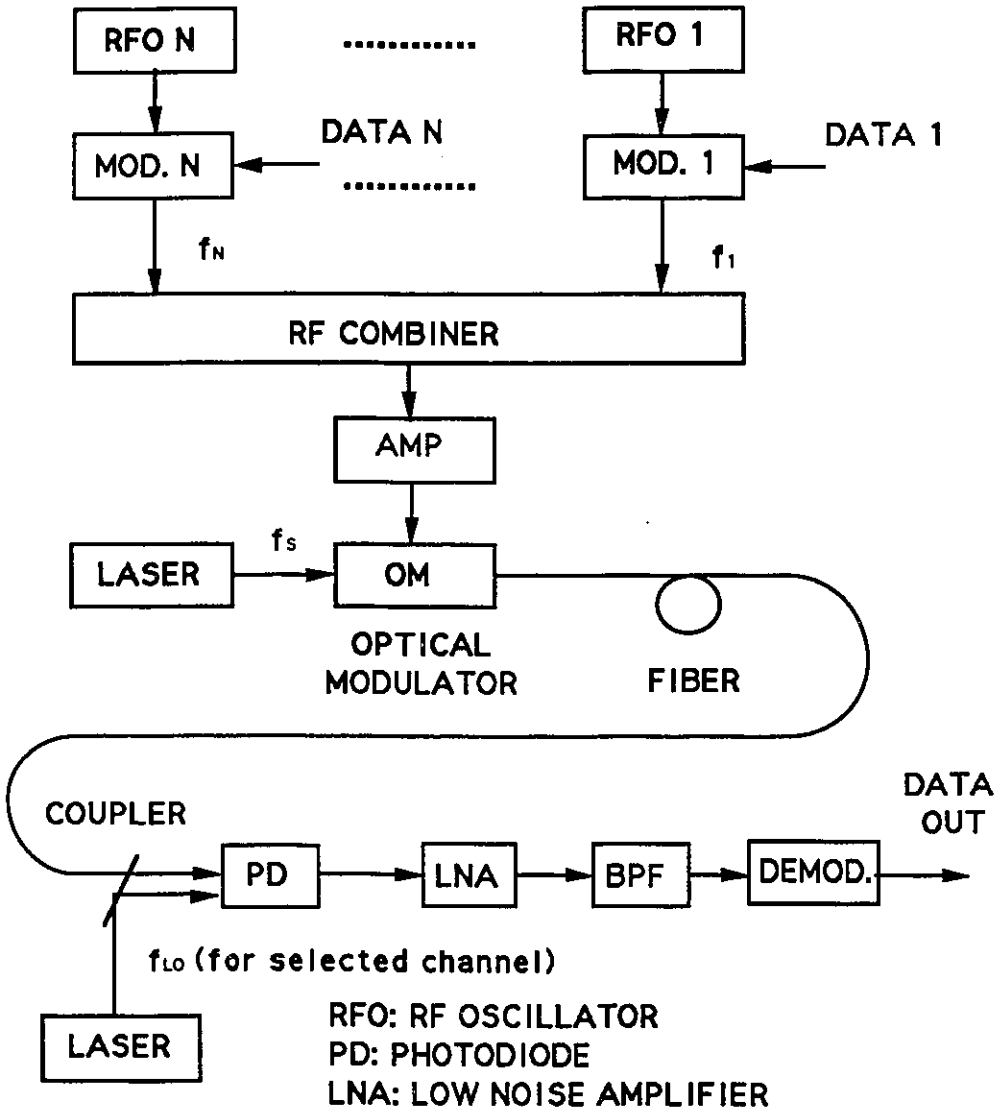

Figure 2.1: Block diagram of an SCM/CD distribution network.

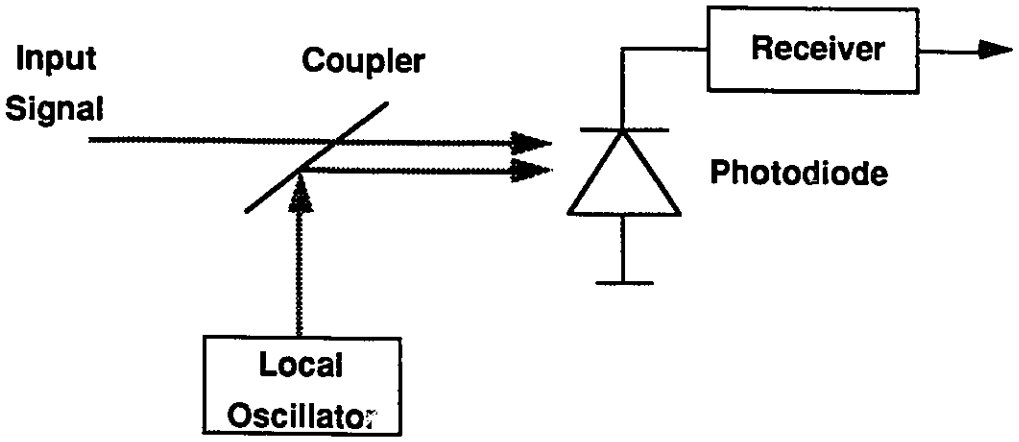

Figure 2.2: Principle of coherent detection.

(LNA) amplifies the output of the detector and the selection of a specific channel is accomplished by optically tuning the local oscillator laser such that the channel is brought inside the passing bandwidth of the bandpass filter. The bandpass filter is used to separate the desired channel from the undesired channels. The signal is then down converted to the RF/microwave domain where it is demodulated using conventional microwave techniques.

The process of photomixing is the key to coherent optical detection. Fig. 2.2 illustrates the principle. The output current of the photodiode is proportional to the square of the amplitude of the incident electrical field of the optical wave.

The electrical field of the received signal $E_s(t)$ and that of the local oscillator $E_{LO}(t)$ can be represented as

$$E_s(t) = \sqrt{P_s(t)}\cos[2\pi f_s t + \phi_s(t) + \theta_s(t)], \tag{2.1}$$

and

$$E_{LO}(t) = \sqrt{P_{LO}(t)}\cos[2\pi f_{LO} t + \phi_{LO}(t) + \theta_{LO}(t)], \tag{2.2}$$

where $P_s(t)$ and $P_{LO}(t)$ are the powers of the transmitted signal and the local oscillator. The variations of $P_s(t)$ and $P_{LO}(t)$ represent the intensity noise; $\theta_s(t)$ and $\theta_{LO}(t)$ represent the phase noise in the transmitted signal and the local oscillator, respectively, and $\phi_s(t)$

and $\phi_{LO}(t)$ are the corresponding phases. The photocurrent will then have the following expression:

$$i(t) = K[E_s(t) + E_{LO}(t)]^2, \tag{2.3}$$

where K is a constant of proportionality.

Since the gain-bandwidth of the photodiode extends only into the gigahertz frequency range, the frequency terms, $2f_s$, $2f_{LO}$ and $f_s + f_{LO}$, in the expansion of (2.3), fall outside of this range and the only detected component will be

$$i(t) = R\left\{P_{LO}(t) + P_s(t) + 2\sqrt{P_{LO}(t)P_s(t)}\cos[2\pi f_{IF}t + \Phi(t) + \theta(t)]\right\} + \eta(t), \tag{2.4}$$

where R (A/W) is the photodiode responsivity, $f_{IF} = f_{LO} - f_s$ is the intermediate frequency, $\Phi(t) = \phi_{LO}(t) - \phi_s(t)$ is the total signal phase, $\theta(t) = \theta_{LO}(t) - \theta_s(t)$ is the total phase noise, and $\eta(t)$ is the additive noise. When $f_{IF} \cong 0$, the receiver is called *homodyne*, and an optical phase locking of the local laser to the incoming signal is necessary. When $f_{IF} \neq 0$, then the receiver is *heterodyne*, and in this case, only frequency locking of the local oscillator laser to the transmitted optical signal is required.

2.1.2 The SCM/CD Multiple-Access Network

The concept of a multiple-access network combining both subcarrier multiplexing and coherent detection was proposed in [5]. This system is illustrated in Fig. 2.3. The network is organized around a passive $M \times M$ star coupler which interconnects M network users. One tunable RF subcarrier frequency is exclusively reserved for each user, and the selection of a particular subcarrier is done by tuning either the local laser, or by tuning an RF oscillator.

The use of an independent transmitter laser at each user location will lead to the problem of beat noise due to the random drift of the laser oscillators. This will result in a severe degradation of the bit-error-rate performance [6, 7]. One of the solutions introduced is the use of a common transmitter laser source [8]. The laser source is connected to one of the input ports of the star coupler and the laser power is evenly distributed among the users through the star network itself.

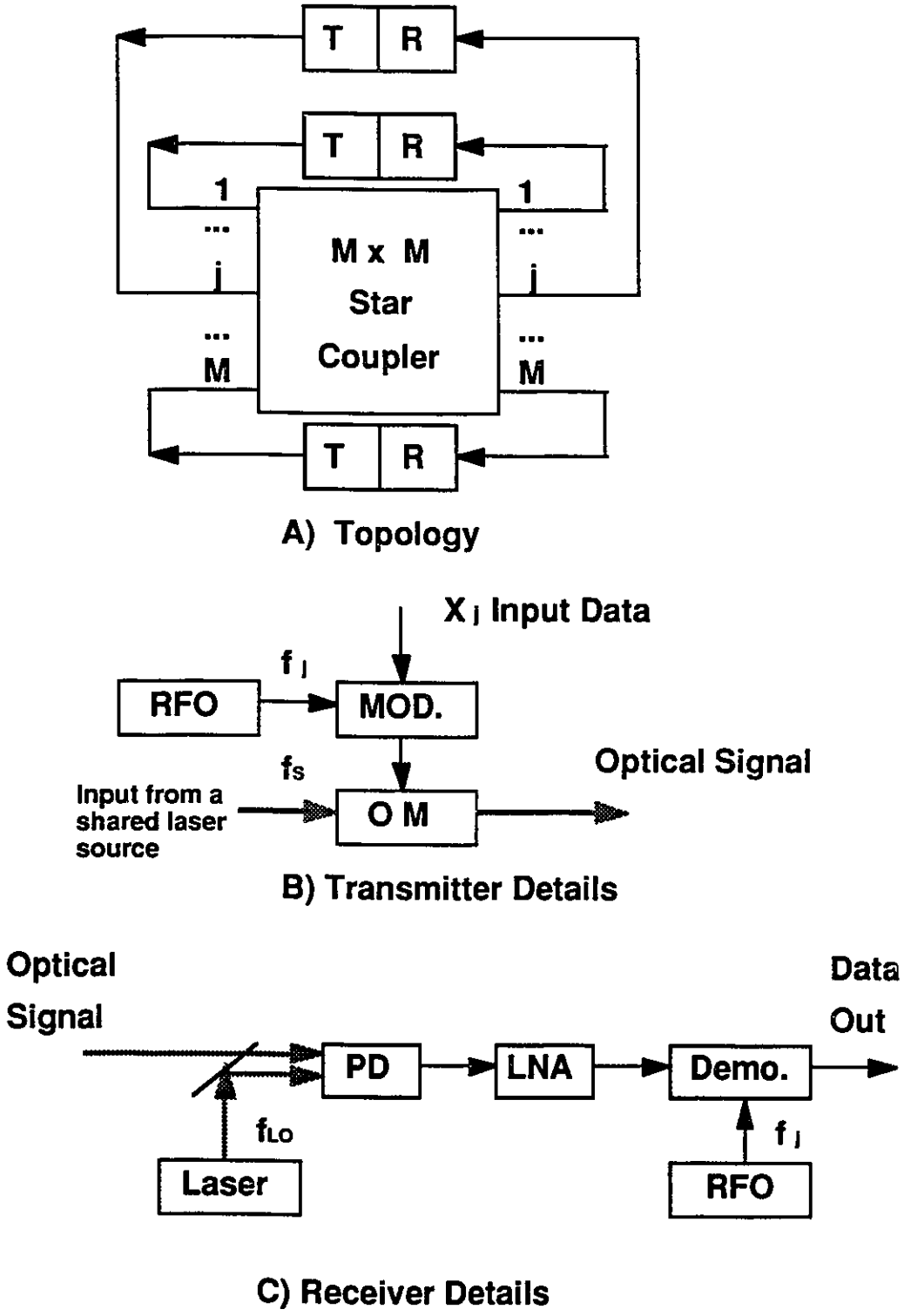

Figure 2.3: Architecture of an SCM/CD multiple-access network.

Since coherent detection is used at the receiver, the major source of shot noise is the local laser. The effect of the excess shot noise produced by the optical power received from all network users remains small as long as the local oscillator power is much stronger compared to that of the received signal [9].

2.2 Problems Associated with SCM/CD Networks

The major problems encountered in SCM/CD networks are those associated with coherent detection. These are laser phase noise, intensity noise and polarization fluctuations. The important problem of laser phase noise will be discussed first. Following this, intensity noise and polarization fluctuations, as well as the main solutions that have been introduced, will be discussed briefly.

2.2.1 Laser Phase Noise

The process of generating photons in a semiconductor is the basis of the operation of laser devices. We need to consider two kinds of photon emission in a laser. First, the stimulated emission where an electron in a higher energy level can be stimulated by a previously created photon to emit a photon which has exactly the same wavelength, direction and phase (coherence) as the stimulating photon. The stimulated emission is amplified with a feedback process leading to a Light Amplification by Stimulated Radiation (LASER). However, there are spontaneous emissions too; in this situation, an electron in a higher energy level emits a photon in a random fashion. Thus, the resulting light will have a random phase.

The stimulated emission process is generally three orders of magnitude faster than the spontaneous process, but the random nature of this latter process results in a light where the phase executes a random walk from its nominal value. Such randomness in the phase is referred to as *phase noise*.

Phase noise is present in all kinds of lasers, however it is stronger in semiconductor lasers. It was found that laser phase noise is also due to fluctuations in the refractive index

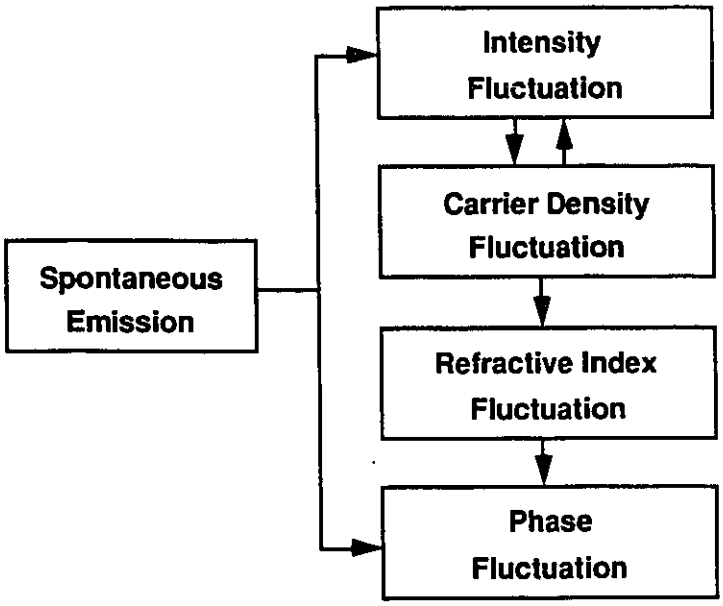

Figure 2.4: Relationship between spontaneous emission, intensity and phase noises, and the carrier density fluctuations.

in the laser cavity, which result from changes in the carrier density [10]. The change in the carrier density causes intensity noise too, which will be discussed in the next section. The relationship between the spontaneous emission, the phase noise and the intensity noise, and the carrier density fluctuations is illustrated in Fig. 2.4 (after [11]). The spontaneous emission is the origin of all these noises and fluctuations.

The lineshape of single-mode semiconductor lasers has been modeled as having a *Lorentzian* power spectral density [12]. The phase noise random process can be expressed as the integral of the frequency noise. It has been observed that the laser frequency noise consists of a white Gaussian noise component plus a $1/f$ component [11, 13]. The latter, because of its lowpass behavior, is significant only up to 1 MHz relatively to the oscillation frequency and is dominated by the white noise component beyond that range of frequencies. Therefore, in the rest of the thesis, only the white component of the laser frequency noise will be considered in our analysis. The phase noise may thus be

characterized by a Wiener process that can be expressed as

$$\theta(t) = 2\pi \int_0^t \mu(\tau) d\tau, \tag{2.5}$$

where $\mu(t)$ (the frequency noise) is a random white Gaussian process with a two-sided spectral density of amplitude N_0. The parameter N_0 is a function of both the laser structure and the operating conditions [13].

The output field of a semiconductor laser can be modeled as the random process

$$s(t) = A\cos[2\pi\nu_0 t + \theta(t) + \phi], \tag{2.6}$$

where ν_0 is the laser oscillation frequency, $\theta(t)$ is the phase noise and ϕ is equally likely to be any value from $[-\pi, \pi]$, as a result of which the process $s(t)$ is stationary. The intensity fluctuations have been neglected. The autocorrelation function of $s(t)$ is then [13]:

$$R_s(\tau) = \frac{A^2}{2}\cos[2\pi\nu_0\tau]\exp\left(-2\pi^2 N_0|\tau|\right). \tag{2.7}$$

Its Fourier transform gives the power spectral density of the laser line:

$$G_s(f) = \frac{A^2}{4\pi^2 N_0}\left[\frac{1}{1+\left(\frac{f-\nu_0}{\pi N_0}\right)^2} + \frac{1}{1+\left(\frac{f+\nu_0}{\pi N_0}\right)^2}\right]. \tag{2.8}$$

This power spectral density (PSD) is called *Lorentzian*. The 3 dB bandwidth of this spectrum around ν_0 is called the full width at half maximum (FWHM) linewidth; it is found to be equal to

$$\Delta\nu = 2\pi N_0. \tag{2.9}$$

The FWHM linewidth is widely used as a measure of the temporal coherence of the laser. For computation purposes, we will use the double-sided baseband version of the laser line PSD, with A normalized to unity:

$$G_{PN}(f) = \frac{1}{\pi\Delta\nu\left[1+\left(\frac{2f}{\Delta\nu}\right)^2\right]}, \quad -\infty < f < +\infty. \tag{2.10}$$

This spectrum is shown in Fig. 2.5.

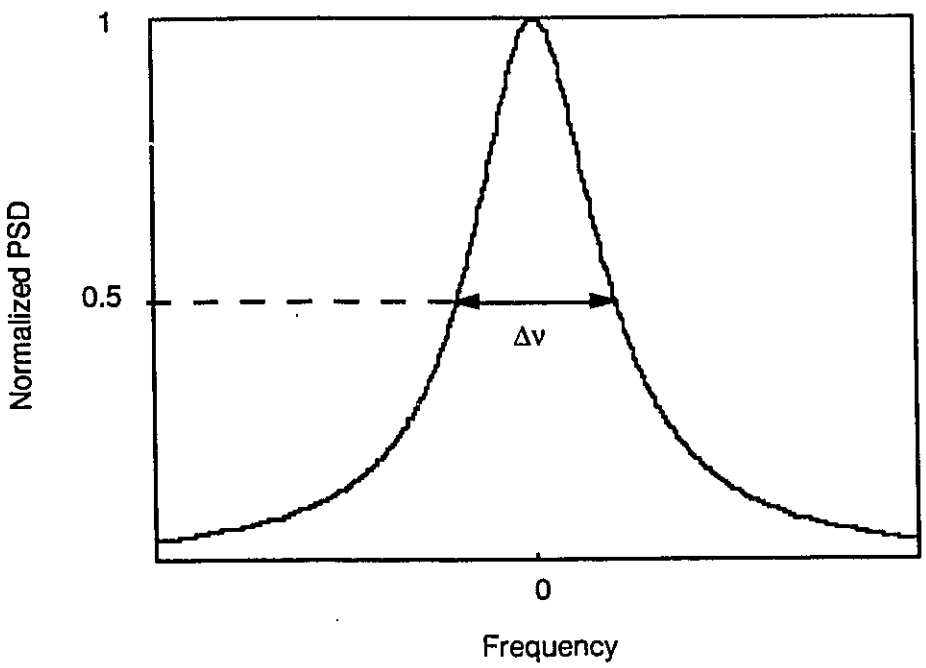

Figure 2.5: Power spectral density of laser line.

The presence of the finite linewidth in the spectrum of the laser output has a direct effect of spectral broadening when the laser is used as an optical carrier. A typical semiconductor laser has a linewidth in the range 1-100 MHz; such a laser source is not coherent enough, i.e., the randomness of the phase of the emitted light is not completely negligible for many important coherent lightwave communication applications. Constant progress is being made in laser device technology, and successful experiments using narrow linewidth NdYAG lasers have been reported [14, 15, 16, 17]. There have been reports of lasers with linewidth as low as 1 KHz [18], but this is accomplished at the expense of compactness and cost.

Several techniques to reduce the effect of laser phase noise have been introduced. Some of them are optimum or suboptimum while others turn to be specific to the kind of modulation scheme used. We will present and discuss those techniques in Chapter 4.

Small size and low power consumption lasers will be essential for future practical coherent communication networks. The best achieved semiconductor laser linewidth is less

than 0.1 MHz [19]. This is obtained by introducing a corrugation-pitch-modulated (CPM) gratings into a multiquantum-well distributed feedback (MQW-DFB) laser. However this narrowing in the laser linewidth is achieved at the expense of an increased complexity and cost.

It is therefore essential to take into account the effect of the laser phase noise in the design of coherent optical networks, and to understand the fundamental limitations set by the phase noise on these systems. In Chapter 3, an attempt to address and analyze these issues in the case of SCM/CD photonic networks is given.

2.2.2 Intensity Noise

The intensity fluctuations present in both the received signal and the local oscillator will be efficiently converted to the IF band and may degrade the receiver's performance. This will be the case if the intensity noise produced is comparable or larger than the quantum shot noise [20].

In addition to the fluctuations in the laser oscillators, the total system intensity noise may be increased due to reflections from fiber discontinuities back into the laser cavity, or by multiple reflections between fiber discontinuities [21]. In such situations, the interference of light beams with different phases will cause the phase noise to be converted into extra intensity noise.

One of the solutions introduced to eliminate, or at least to reduce, the degradation from intensity noise is the balanced mixer receiver [20, 22, 23]. A block diagram of such a receiver is shown in Fig. 2.6. Both of the coupler's outputs are separately detected; the IF signals in the two detectors are 180° out of phase, while the intensity noise produced in each detector is in phase. Thus, a subtraction of the two photocurrents eliminates the DC components that carry intensity fluctuations. However, to realize a complete cancellation of the intensity noise, a perfect matching of the detector frequency responses and the optical or electrical path lengths in the two branches of the receiver is required.

It was found in [20] that for a 20 dB reduction in the intensity noise introduced by the local oscillator the following requirements should be satisfied: the signal path lengths

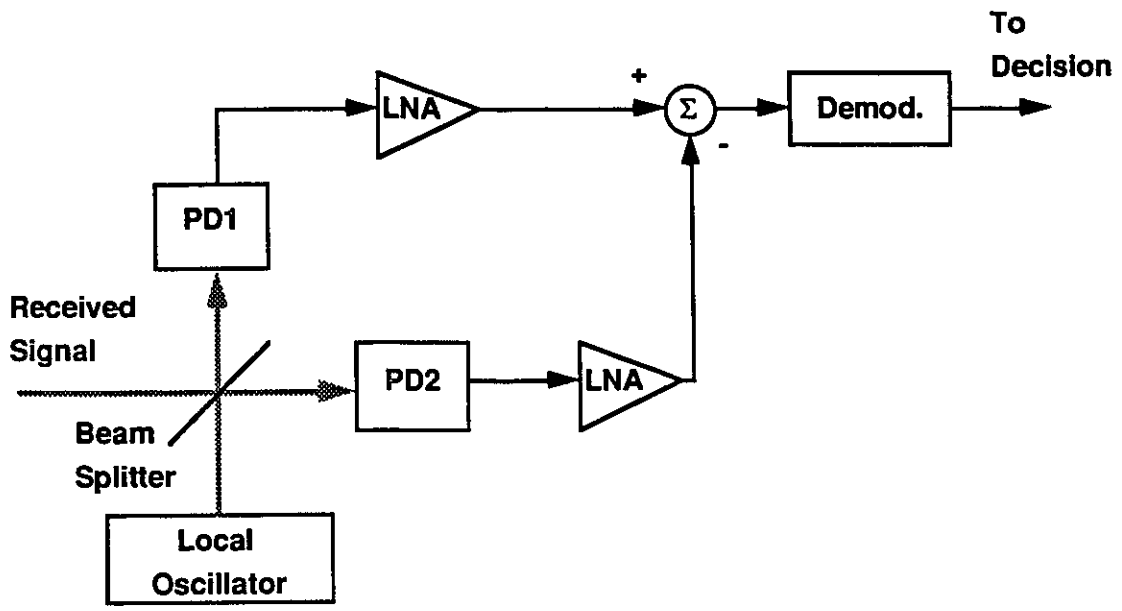

Figure 2.6: Balanced mixer receiver model.

should be matched to within a few millimeters and a maximum of 1 dB mismatch between the photodetectors, in terms of quantum efficiency and frequency response, for a 1 GHz receiver.

In the case of SCM/CD networks, or multi-channel networks in general, a balanced optical mixer is also needed to eliminate the interference from mixing between channels [9].

2.2.3 Polarization Fluctuations

In ordinary single-mode fibers, two orthogonal polarization modes are supported; because actual optical fibers suffer from axial asymmetry and are not completely straight, the state of polarization of the propagated wave is subject to unstable fluctuations resulting from temperature changes.

In coherent communications, the state of polarization of the received signal and that of the local oscillator must match for efficient photo-mixing [24]. Furthermore, for multi-channel networks, the acquisition of polarization would limit switching times, so it

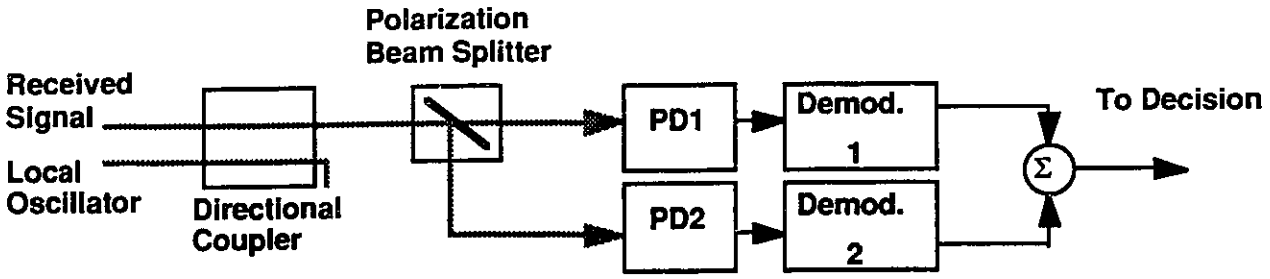

Figure 2.7: Polarization-diversity receiver.

is desirable to design receivers that are insensitive to the state of polarization [1].

The complete solution to this problem is the use of a polarization-maintaining fiber over the entire length of the communication channel; such a solution would be very expensive at the present technological stage of the development of these fibers.

Polarization control schemes have been introduced; two alternatives have been proposed. Automatic polarization compensation schemes, based on electro-optic or mechanical devices, which matches the local oscillator and received signal states of polarization [25, 26, 27, 28]. A description and details on these techniques can be found in [11].

Another approach is the polarization-diversity receivers in which two orthogonal polarization states are detected separately and added later [29, 30]. The general idea of this technique is illustrated in Fig. 2.7. The two independent channels fade in opposite directions which makes the signal at the output of the receiver independent of the state of polarization of the received signal.

The analysis of some polarization-diversity receivers showed that the receiver sensitivity penalty was less than 0.6 dB as compared to the ideal case of a perfect polarization controller [30].

In addition, various versions and combinations of the previous techniques can be implemented.

Chapter 3

The Impact of Laser Phase Noise on SCM/CD Networks

3.1 Introduction

In Chapter 2, the concept of SCM/CD networks has been introduced and two kinds of networks have been presented, the distribution network and the multiple-access network.

There have been a number of papers on subcarrier multiplexed systems with coherent detection (SCM/CD Systems) [14, 15, 16, 17, 31, 32]. A theoretical comparison of optical phase modulation (OPM) and optical intensity modulation (OIM) with negligible laser phase noise was carried out [31]. Recently, the impact of laser phase noise on an SCM/CD system using OPM was presented [32]. In that paper the performance degradation due to phase noise was analyzed in terms of the carrier-to-noise ratio penalty and the SCM/CD distribution network was considered only.

In this chapter, the effect of laser phase noise on the two types of SCM/CD networks is investigated. As it was found that the receiver sensitivity is a more useful measure of performance than the carrier-to-noise ratio [31], the analysis is carried out, for both OPM and OIM, in terms of the receiver sensitivity penalty. The investigation gives the range of possible linewidths for SCM/CD networks and shows how the optical modulation format influences the performances of the networks in the presence of laser phase noise.

A comparison of the performance of the networks is presented and the range of acceptable laser linewidths is derived in each case. Finally, a discussion is given on the possible number of network users and how that number depends on the laser phase noise.

3.2 Optical Modulation Formats

Coherent communication techniques allow alternative optical modulation formats to the direct intensity modulation of the laser; angle modulation is thus feasible. The spectral selectivity in coherent optical detection being an important feature, it is essential that the individual channels, for instance the subcarriers in SCM/CD networks, be separated in the optical domain as well as in the microwave domain. This is necessary since two kinds of modulation are applied one on top of the other: a microwave modulation plus an optical modulation.

The main task of the optical modulation technique is to create optical sidebands carrying the information. Amplitude modulation would be the most suitable format for optical modulation, since by its nature it preserves the spectrum of the information signal; unfortunately, true optical AM modulation has not been demonstrated yet [5].

Optical intensity modulation (OIM) is used as a mean to approach the performance of AM modulation; the laser injection current is modulated by the information signal, the resulting output power will vary accordingly. However, direct modulation of the injection laser bias will cause optical frequency modulation due to a change in the carrier density and this will be difficult to suppress [1]. For this reason, an external electro-optic modulator is used to impress the data on the optical carrier.

The electro-optic modulator takes advantage of the electro-optic Pockel's effect which is a result of the linear relationship that exists between the applied voltage across the electrodes attached to a crystal and the induced phase shift in the light propagating through the crystal [33]. In Fig. 3.1 is illustrated a diagram of a Mach-Zehnder interferometer intensity modulator (after [33]). The optical input signal is split between parallel waveguides. A phase shift, proportional to the applied voltage, is introduced in one of

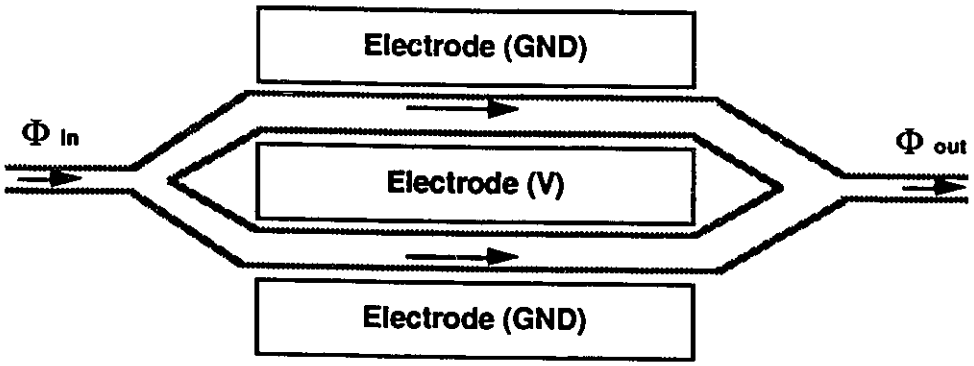

Figure 3.1: Mach-Zehnder interferometer intensity modulator.

the waveguides; then, the two signals are summed together at the output where they undergo destructive interference. Thus, the intensity of the optical output signal could be controlled by the applied voltage.

The modulator output light intensity, or optical power, is given by [33, 34, 35, 36]:

$$P_{out}(t) = P_{in}(t) \sin^2 \left[\frac{\pi}{2} \frac{v(t)}{V_\pi} \right], \tag{3.1}$$

where P_{out} is the output light intensity, P_{in} is the input intensity, $v(t)$ is the applied voltage, i.e., the signal carrying information, and V_π is the voltage that causes a shift of π of the light passing through the modulator.

Another modulation format is used in coherent detection; it is the optical phase modulation (OPM). The phase of the laser light beam, instead of its intensity, is changed in accordance with the information signal. An external phase modulator is needed here too. Its structure is similar to the waveguide of the intensity modulator where phase shift is introduced. The applied voltage introduces a change in the refractive index of the waveguide, which in turn will alter the velocity of the light passing through the waveguide and causes phase modulation.

Both OPM and OIM are inherently nonlinear, and the associated distortion, the intermodulation distortion, will degrade the system performance. Furthermore, the degra-

dation gets worse in the presence of laser phase noise as will be seen later in this chapter.

While in multi-channel SCM systems using direct detection (SCM/DD systems), the main source of nonlinearity is the laser itself, the nonlinearity of the optical modulation and the coherent detection process are dominant in SCM/CD systems and will place an ultimate limit on the achievable receiver sensitivity [17].

3.3 Laser Phase Noise and its Effect on the SCM/CD Distribution Network

The power spectrum of the signal in an N-channel multicarrier SCM/CD distribution network receiver, at the input of the bandpass filter (see Fig. 2.1) is illustrated in Fig. 3.2. The subcarrier frequencies are

$$f_k = [(k - \frac{1}{2}) + N_{min}]\Delta f, \tag{3.2}$$

where k is the channel number, $k = 1, 2, ..., N$; N_{min} is an integer related to the smallest subcarrier frequency of the system $f_{min} = f_1 = [\frac{1}{2} + N_{min}]\Delta f$, and Δf is the channel spacing. Such a frequency allocation minimizes the effect of second-order intermodulation distortion (IMD_2), in that its spectrum falls in between the channels. However, third-order intermodulation distortion (IMD_3) will directly affect each channel as shown in Fig. 3.2.

The number of IMD_2 terms depends on whether we operate in single-octave (SO), or in multi-octave (MO). In SO operation, the subcarriers span one octave of frequency, i.e., for $k = N$, $f_N \leq 2f_1$ and thus we should have $N_{min} \geq N$. In MO operation, where $N_{min} < N$, the number of IMD_2 terms of the form $f_i \pm f_j$, $i, j = 1, 2, ..., N$ and $i \neq j$, that affect channel k is given by [32]

$$P_2(k) = \begin{cases} \Lambda_2(k), & k = N - N_{min} \text{ or } k = N_{min} + 1; \\ \Lambda_2(k) + \Lambda_2(k+1), & \text{otherwise;} \end{cases} \tag{3.3}$$

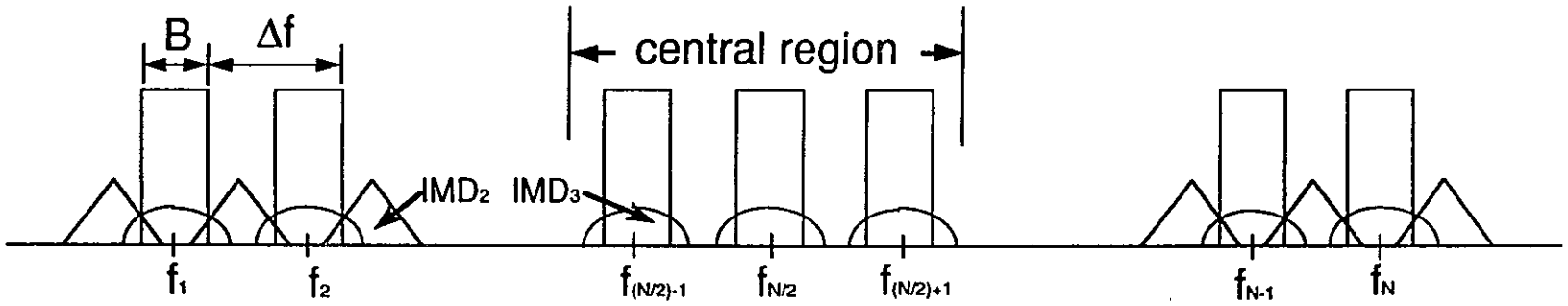

Figure 3.2: Power spectrum of the signal in an SCM/CD distribution network at the input of the bandpass filter.

where $\Lambda_2(k)$, the number of IMD_2 falling between channels $(k-1)$ and k, is

$$\Lambda_2(k) = \begin{cases} N+1-N_{min}-k, & 1 \le k \le N-N_{min}; \\ 0, & N-N_{min}+1 \le k \le N_{min}+1; \\ \lfloor \frac{1}{2}(k-N_{min}-1) \rfloor, & N_{min}+2 \le k \le N; \end{cases} \tag{3.4}$$

where $\lfloor X \rfloor$ is the largest integer not greater than X. In the case of SO operation there is no IMD_2 falling in the operating bandwidth, therefore

$$P_2(k) = 0. \tag{3.5}$$

The number of IMD_3 terms of the form $f_i \pm f_j \pm f_k$, $i,j,k = 1,2,...,N$ and $i \neq j \neq k$, for both MO and SO is [32]

$$P_3(k) = \frac{k}{2}(N-k+1) + \frac{1}{4}[(N-3)^2 - 5]. \tag{3.6}$$

3.3.1 The Effect of Laser Phase Noise

When the channel is corrupted by laser phase noise, the power spectrum of the signal is broadened. It has been shown that the contaminated spectrum is given by the convolution of the signal power spectrum $S_k(f)$ and the power spectrum of the laser line $G_{PN}(f)$ [37]:

$$S_{k_{PN}}(f) = S_k(f) * G_{PN}(f), \tag{3.7}$$

where

$$S_k(f) = \begin{cases} 1, & f_k - \frac{B}{2} \le f \le f_k + \frac{B}{2}\ ; \\ 0, & \text{otherwise;} \end{cases} \tag{3.8}$$

B is the receiver bandwidth when the laser phase noise is negligible, and $G_{PN}(f)$ is as given in (2.10).

Thus

$$\begin{aligned} S_{k_{PN}}(f) &= 2\int_{f-f_k-\frac{B}{2}}^{f-f_k+\frac{B}{2}} \left\{ \pi\Delta\nu \left[1 + \left(\frac{2x}{\Delta\nu} \right)^2 \right] \right\}^{-1} dx \\ &= \frac{1}{\pi} \left\{ \tan^{-1}\left[\frac{2(f-f_k)+B}{\Delta\nu} \right] - \tan^{-1}\left[\frac{2(f-f_k)-B}{\Delta\nu} \right] \right\}. \end{aligned} \tag{3.9}$$

In the above derivation, we have assumed an ideal rectangular signal power spectrum for each uncontaminated channel. The quantity $\Delta\nu$ in (3.9) represents now the FWHM linewidth at the intermediate frequency (IF), i.e., the sum of the transmitter and the local oscillator laser linewidths.

In Fig. 3.3 is illustrated the power spectrum of the signal in a channel corrupted by phase noise, for several values of the normalized laser linewidth $\Delta\nu/B$.

Since the effect of the phase noise is to broaden the signal spectrum in each channel, the bandwidth of the bandpass filter at the receiver should be increased to avoid distortion. We define $B_{IF}(\Delta\nu)$ as the bandwidth necessary to accommodate 95% of the power of the signal in the contaminated channel:

$$\int_{f_k-\frac{B_{IF}(\Delta\nu)}{2}}^{f_k+\frac{B_{IF}(\Delta\nu)}{2}} S_{k_{PN}}(f)df = 0.95\int_{-\infty}^{+\infty} S_{k_{PN}}(f)df. \tag{3.10}$$

The variations of the normalized bandwidth $B_{IF}(\Delta\nu)/B$ with respect to the normalized laser linewidth $\Delta\nu/B$ are shown in Fig. 3.4.

3.3.2 Optical Phase Modulation (OPM)

The received photo-current in an SCM/CD network is given by (2.4),

$$i(t) = R\left\{P_{LO} + P_s(t) + 2\sqrt{P_{LO}P_s(t)}\cos[2\pi(f_s - f_{LO})t + \Phi(t) + \theta(t)]\right\} + \eta(t) \tag{3.11}$$

where R is the photodiode responsivity, P_{LO} is the local laser oscillator power, $P_s(t)$ is the received signal power, f_s is the optical carrier frequency, f_{LO} is the local laser oscillator frequency, $\Phi(t)$ is the modulated optical carrier phase, $\theta(t)$ is the phase noise, and $\eta(t)$ is the additive noise. When OIM is used, the phase $\Phi(t)$ is fixed (beside the residual chirp the intensity modulator may have), whereas in OPM, the received optical signal power $P_s(t)$ is constant. In the latter case, the N subcarriers modulate the phase as follows:

$$\Phi(t) = \sum_{k=1}^{N} \beta_k \cos[2\pi f_k t + x_k(t)], \tag{3.12}$$

where β_k is the individual phase modulation index of the kth subcarrier, at frequency f_k, and $x_k(t)$ is the information signal modulating the kth subcarrier.

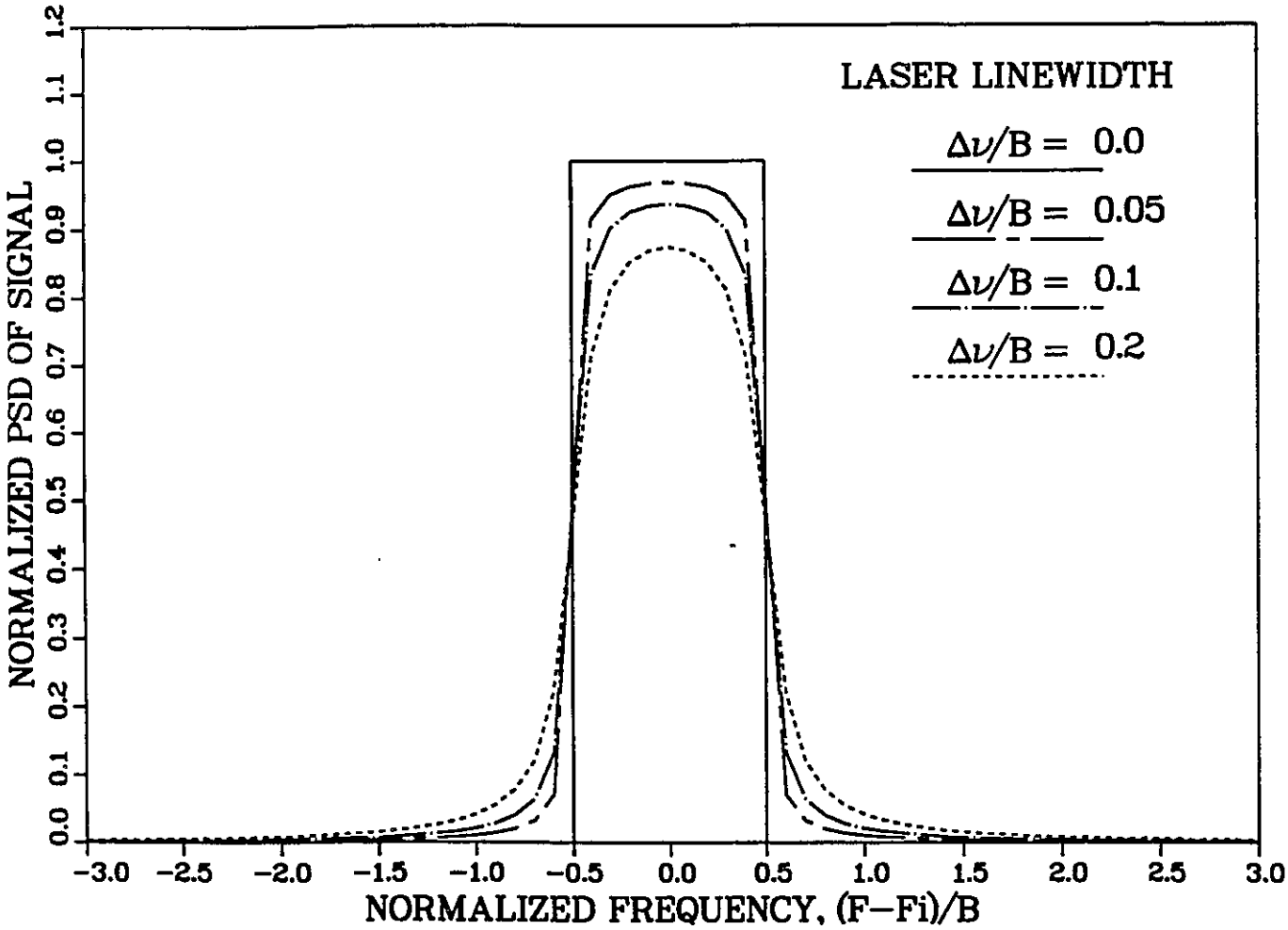

Figure 3.3: Power spectrum of the signal in a contaminated channel.

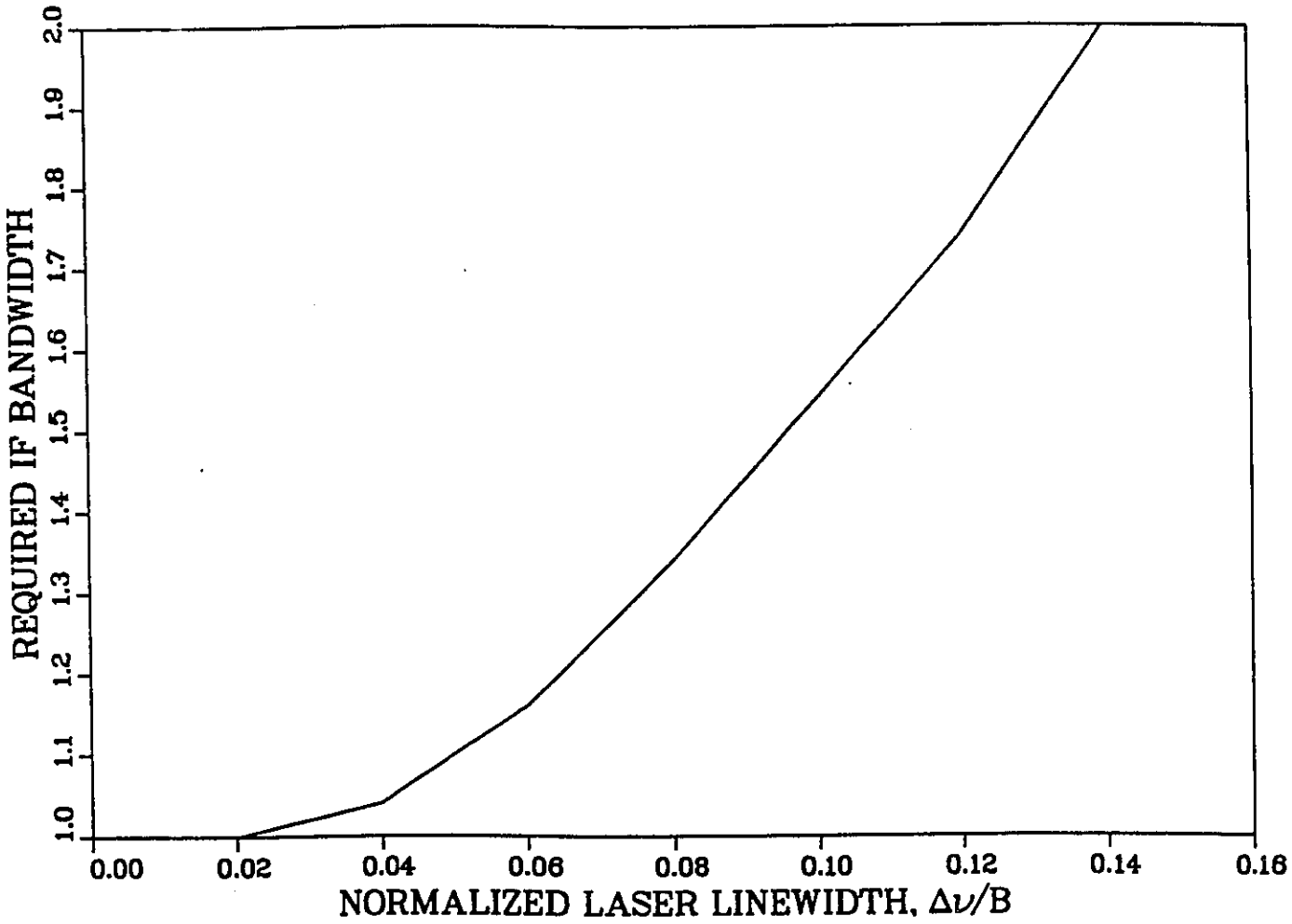

Figure 3.4: Normalized IF bandwidth $\frac{B_{IF}(\Delta\nu)}{B}$ necessary to accommodate 95% of the signal power as a function of the normalized laser linewidth $\frac{\Delta\nu}{B}$.

The information signal, as seen in Section 2.1.1, could be either an analog or a digital signal. One of the modulation schemes that has gained popularity is FSK [15, 16, 17, 31, 37, 38]. The reason is that FSK offers a better discrimination against noise and interference than other digital modulation techniques, and allows for the use of asynchronous demodulator receivers (e.g., the "delay and multiply" receiver) which are simple and less expensive. Also, the increase in the required bandwidth by FSK can be accommodated in a fiber-optic system. This makes FSK probably the simplest technique for multiple-access network applications [39].

The use of continuous-phase FSK (CPFSK) is preferred [37]; it is chosen here also. The signal modulating the subcarrier will be in that case

$$x_k(t) = 2\pi f_d \int_{-\infty}^{t} \sum_i a_i g(\tau - iT) d\tau, \tag{3.13}$$

where f_d is the peak frequency deviation, a_i the binary information, $g(t)$ a rectangular pulse, and T the bit period.

Assuming that all subcarriers have the same phase modulation index β, and ignoring the DC terms in (3.11), which do not carry information, the received photocurrent can be expanded as follows [17]:

$$\begin{aligned} i_{PM}(t) \;=\; & 2R\sqrt{P_{LO}P_s} \sum_{n_1=-\infty}^{+\infty} \cdots \sum_{n_N=-\infty}^{+\infty} J_{n_1}(\beta) \ldots J_{n_N}(\beta) \cos\,[2\pi f_{IF} t + \\ & n_1(2\pi f_1 t + x_1(t)) + \ldots + n_N(2\pi f_N t + x_N(t)) + \theta(t)] + \eta(t), \end{aligned} \tag{3.14}$$

where $f_{IF} = (f_s - f_{LO})$ is the intermediate frequency and $J_n(\beta)$ is an nth order Bessel function of the first kind.

In heterodyne detection, only one of the optical sidebands is used and the signal for the kth channel is obtained by setting index $n_k = -1$ and the remaining indices to zero:

$$i_{k_{PM}}(t) = 2R\sqrt{P_{LO}P_s} J_1(\beta)[J_0(\beta)]^{N-1} \cos[2\pi(f_{IF} - f_k)t - x_k(t) + \theta(t)], \tag{3.15}$$

and the effective optical AM index is

$$m_{e_{PM}} = J_1(\beta)[J_0(\beta)]^{N-1}. \tag{3.16}$$

From (3.15), the carrier-to-noise ratio (CNR) is then,

$$\text{CNR} = \frac{2R^2 P_{LO} P_s {J_1}^2(\beta)[J_0(\beta)]^{2N-2}}{\sigma_{sh}^2 + \sigma_{th}^2 + \sigma_{2d}^2 + \sigma_{3d}^2 + \sigma_{ct}^2}, \tag{3.17}$$

where noise terms in the denominator are [17]:

(i) $\sigma_{sh}^2 = 2qRP_{LO}B_{IF}(\Delta\nu)$ is the shot noise power (q is the electron charge);

(ii) $\sigma_{th}^2 = KTF_N B_{IF}(\Delta\nu)/R_L$ is the thermal noise power (K is Boltzmann's constant, T is the absolute temperature of the receiver, F_N is the receiver noise figure and R_L is the receiver load resistance);

(iii) σ_{ct}^2 is the adjacent-channel crosstalk noise power (It could be neglected with sufficiently wide channel spacing. When CPFSK is used for the information signal, a subcarrier separation of twice the bit rate is generally enough to avoid interchannel interference [39]);

(iv) $\sigma_{2d}^2 = 2R^2 P_{LO} P_s h_2(\Delta\nu) P_2(k) {J_1}^4(\beta)[J_0(\beta)]^{2N-4}$ is the variance of the second-order distortion; and

(v) $\sigma_{3d}^2 = 2R^2 P_{LO} P_s h_3(\Delta\nu) P_3(k) {J_1}^6(\beta)[J_0(\beta)]^{2N-6}$ is the variance of the third-order distortion.

The quantities $h_2(\Delta\nu)$ and $h_3(\Delta\nu)$ are coefficients that are the fractions of IMD_2 and IMD_3 powers respectively that remain in the bandpass filter output in the receiver. The details on the evaluation of these coefficients are given in Appendix A. As shown in Appendix A, the corresponding expressions are

$$h_2(\Delta\nu) = \begin{cases} \frac{1}{8}\left[3 - \frac{\Delta f}{B_{IF}(\Delta\nu)}\right]^2, & \Delta f \le 3B_{IF}(\Delta\nu); \\ 0, & \Delta f > 3B_{IF}(\Delta\nu); \end{cases} \tag{3.18}$$

and

$$h_3(\Delta\nu) = 1 - \left[1 - \frac{B_{IF}(\Delta\nu)}{3B}\right]^3. \tag{3.19}$$

A graphical interpretation of (3.18) and (3.19) is given in Fig. 3.5. As the laser linewidth increases, both coefficients increase and this is a direct consequence of the necessary increasing of the IF bandwidth, since this results in more IMD's power into the receiver. Throughout our analysis, we have assumed all the noise sources to be Gaussian.

The optimum phase modulation index β_{opt} for each channel is obtained by maximizing the receiver sensitivity, which is equivalent to minimizing P_s for a given CNR that

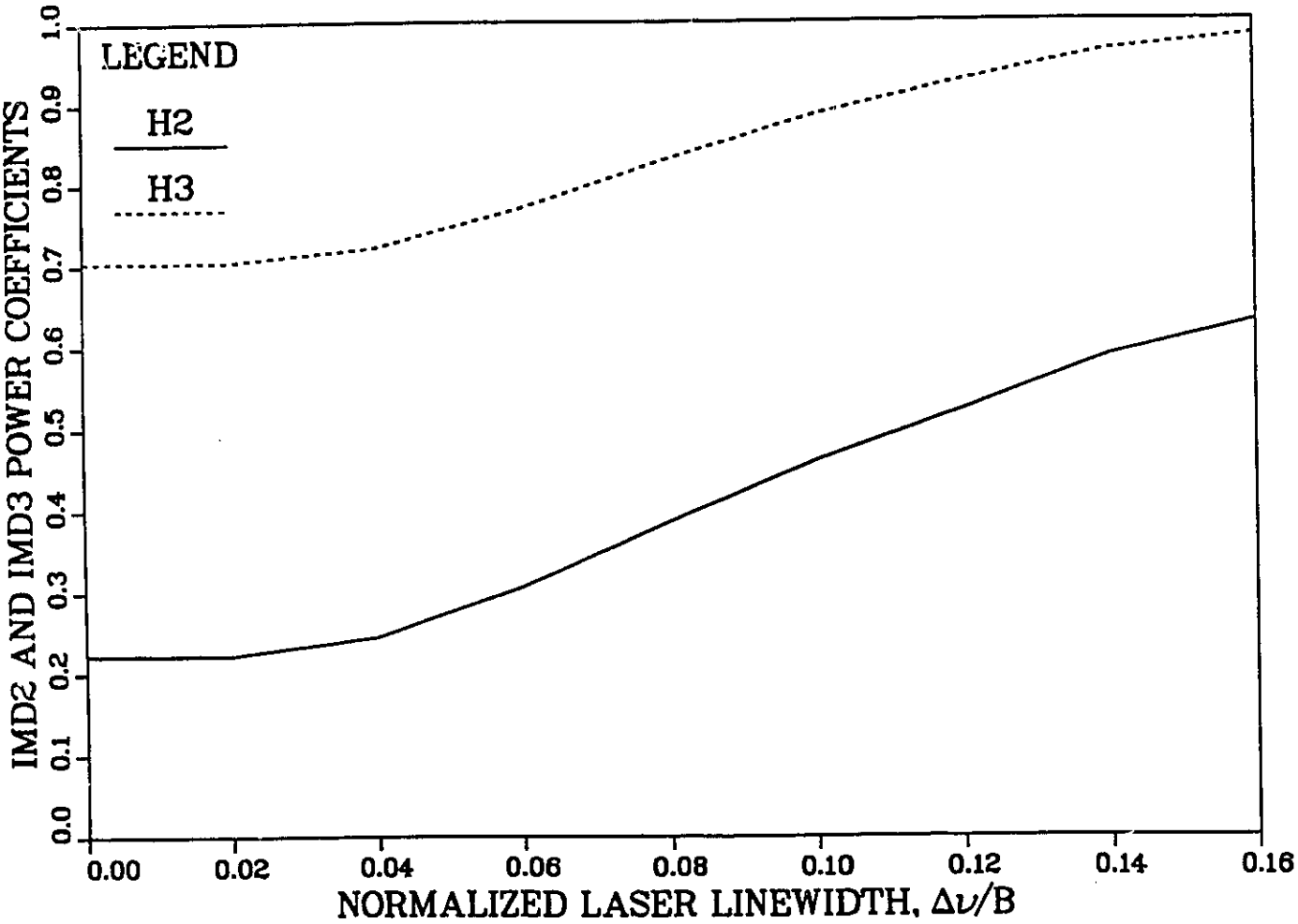

Figure 3.5: Variations of the IMD's power coefficients h_2 and h_3 with respect to the normalized laser linewidth $\frac{\Delta\nu}{B}$.

would be enough to produce a BER of 10^{-9}. For that purpose, we linearize (3.17) by setting, for small β, $J_0(\beta) \approx 1$ and $J_1(\beta) \approx \beta/2$ and solve it for P_s:

$$P_s(\Delta\nu) = \frac{2[\sigma_{sh}^2 + \sigma_{th}^2]}{R^2 P_{LO}\left[\frac{\beta^2}{CNR} - h_2(\Delta\nu)P_2(k)\frac{\beta^4}{4} - h_3(\Delta\nu)P_3(k)\frac{\beta^6}{16}\right]}. \tag{3.20}$$

By equating the partial derivative with respect to β to zero, we get the following equation:

$$-\frac{2}{\mathrm{CNR}} + h_2(\Delta\nu)P_2(k)\beta^2 + \frac{3}{8}h_3(\Delta\nu)P_3(k)\beta^4 = 0. \tag{3.21}$$

The solution of (3.21) yields the optimum optical phase modulation index

$$\beta_{opt} = \left[\frac{-4h_2(\Delta\nu)P_2(k) + \left[16\{h_2(\Delta\nu)P_2(k)\}^2 + \frac{48h_3(\Delta\nu)P_3(k)}{CNR}\right]^{\frac{1}{2}}}{3h_3(\Delta\nu)P_3(k)}\right]^{\frac{1}{2}}. \tag{3.22}$$

The optimum phase modulation index as a function of the laser linewidth for the multi-octave mode of operation and for the same system parameters as in the experiment reported in [17] is given in Fig. 3.6. The system parameters are summarized in Table 3.1 and will be used in the rest of the thesis as the typical system parameters in our analysis. For negligible laser linewidths, the results are consistent with [17]; when the phase noise starts to affect the performance of the system, the phase modulation index should be decreased.

When operating in single-octave, this result simplifies to

$$\beta_{opt} = \frac{2}{[3h_3(\Delta\nu)P_3(k)CNR]^{\frac{1}{4}}}. \tag{3.23}$$

If we combine equations (3.20) and (3.21), we get the expression for the optimum receiver sensitivity:

$$P_{s_{opt}}(\Delta\nu) = \frac{16[\sigma_{sh}^2 + \sigma_{th}^2]}{R^2 P_{LO}[2h_2(\Delta\nu)P_2(k)\beta_{opt}^4 + h_3(\Delta\nu)P_3(k)\beta_{opt}^6]}. \tag{3.24}$$

The receiver sensitivity penalty due to phase noise is defined as

$$\Delta P_s(\text{in dB}) = 10\log\frac{[P_{s_{opt}}(\Delta\nu)]}{[P_{s_{opt}}(\Delta\nu = 0)]}. \tag{3.25}$$

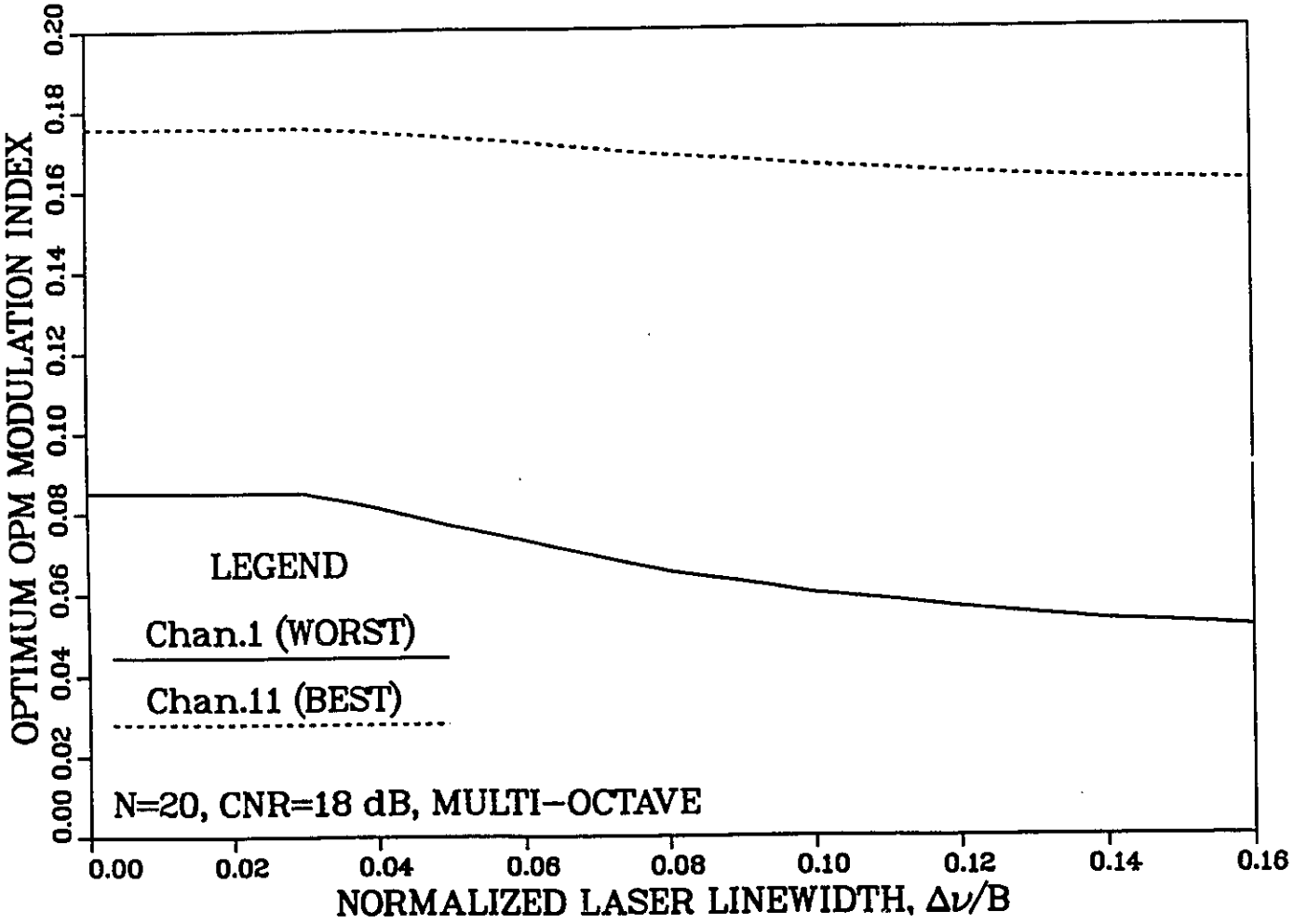

Figure 3.6: Optimal OPM index versus laser linewidth for the the best and worst channels. Multi-octave operation, N=20.

Parameter	Value	Units	Meaning
N	20		Number of channels
R_b	100	Mb/s	Bit-rate per channel
Δf	200	MHz	Channel spacing
$m = 2f_dT$	0.75		FSK index
B	120	MHz	Receiver bandwidth for negligible laser linewidth
F_N	3.8	dB	Receiver noise figure
R_L	50	Ohm	Receiver Load Resistance
P_{LO}	0	dBm	Local laser oscillator power
λ	1.3	μm	Wavelength of operation

Table 3.1: System parameters for numerical calculations

3.3.3 Optical Intensity Modulation (OIM)

The applied voltage in (3.1) could be written as

$$v(t) = \alpha\frac{V_\pi}{2} + V_m y(t), \tag{3.26}$$

where α is the external modulator bias coefficient, when $\alpha = 1$ the modulator output power is half the maximum; V_m is the voltage amplitude of each subcarrier, all assumed to have equal values, and $y(t)$ is the sum of N modulated subcarriers each of unit amplitude:

$$y(t) = \sum_{j=1}^{N} \cos[2\pi f_j t + x_j(t)]. \tag{3.27}$$

The received optical power in (3.1) can then be expressed as

$$P_s(t) = P_m \sin^2\left[\frac{\alpha\pi}{4} + \frac{\pi}{2}\frac{V_m}{V_\pi}y(t)\right], \tag{3.28}$$

where P_m is the hypothetical maximum optical power received.

In the expression for the receiver photocurrent (3.11), both the root-mean-square amplitude of the electrical field of the optical wave $\sqrt{P_s(t)}$ and its intensity $P_s(t)$ are

detected. The voltage-intensity (3.28) and amplitude-intensity (root-square of the expression in (3.28)) curves of the external intensity modulator are shown in Fig. 3.7. It can be seen that the latter characteristic, unlike the former, does not have an inflection point which would eliminate the second order distortion. Furthermore, the linear zone of the voltage-amplitude curve is at lower bias voltages, while the dynamic range of the system is restricted when reducing α or equivalently the bias voltage. For these reasons, the modulator bias α should be optimized.

The distortion inherent to OIM can be expressed by expanding the amplitude of the electrical field of the optical wave into a power series [5]:

$$\begin{aligned}\sqrt{P_s(t)} &= \sqrt{P_m}\left\{\sin\left(\frac{\alpha\pi}{4}\right) + m_{e_I} y(t)\cos\left(\frac{\alpha\pi}{4}\right) - \frac{1}{2!}[m_{e_I}]^2 \right. \\ &\quad \left. \sin\left(\frac{\alpha\pi}{4}\right) + \frac{1}{3!}[m_{e_I}]^3\cos\left(\frac{\alpha\pi}{4}\right) + ...\right\}, \end{aligned} \tag{3.29}$$

where

$$m_{e_I} = \frac{\pi}{2}\frac{V_m}{V_\pi} \tag{3.30}$$

is the effective optical AM index. Ignoring the terms of order higher than three and combining (3.11) and (3.29), we get the expression for the receiver photocurrent:

$$\begin{aligned}i_{IM}(t) &= RP_s(t) + 2R\sqrt{P_{LO}P_m}\left\{\sin\left(\frac{\alpha\pi}{4}\right) + m_{e_I} y(t)\cos\left(\frac{\alpha\pi}{4}\right) - \frac{1}{2!}[m_{e_I}]^2 \right. \\ &\quad \left. \sin\left(\frac{\alpha\pi}{4}\right) + \frac{1}{3!}[m_{e_I}]^3\cos\left(\frac{\alpha\pi}{4}\right)\right\}\cos[2\pi f_{IF}t + \theta(t)] + \eta(t), \end{aligned} \tag{3.31}$$

where $\theta(t)$ is again the laser phase noise and $\eta(t)$ is the additive noise.

As shown in Chapter 2, the selection of a specific channel, say the kth channel, is done by tuning the local oscillator laser so that the channel frequency $(f_{IF} - f_k)$ coincides with the central frequency of the bandpass filter. After neglecting the direct detection term $RP_s(t)$ (which is weak in comparison to the IF term), the term that contains the signal for the kth channel is

$$i_{k_{IF}}(t) = 2R\sqrt{P_{LO}P_m}m_{e_I}\cos\left(\frac{\alpha\pi}{4}\right)\cos[2\pi f_{IF}t + \theta(t)]\cos[2\pi f_k t + x_k(t)]. \tag{3.32}$$

The bandpass filter will pass only the difference term and the signal for the kth channel

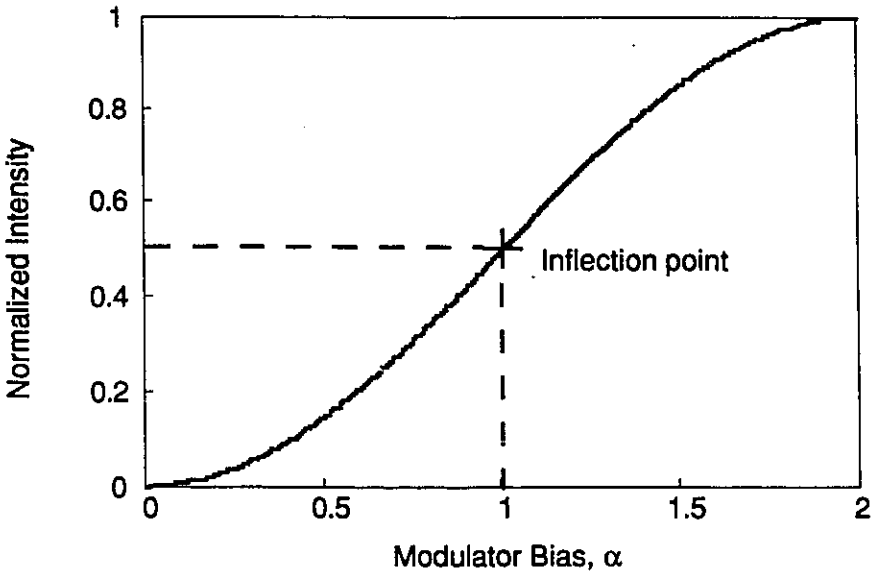

a) Voltage-Intensity Curve.

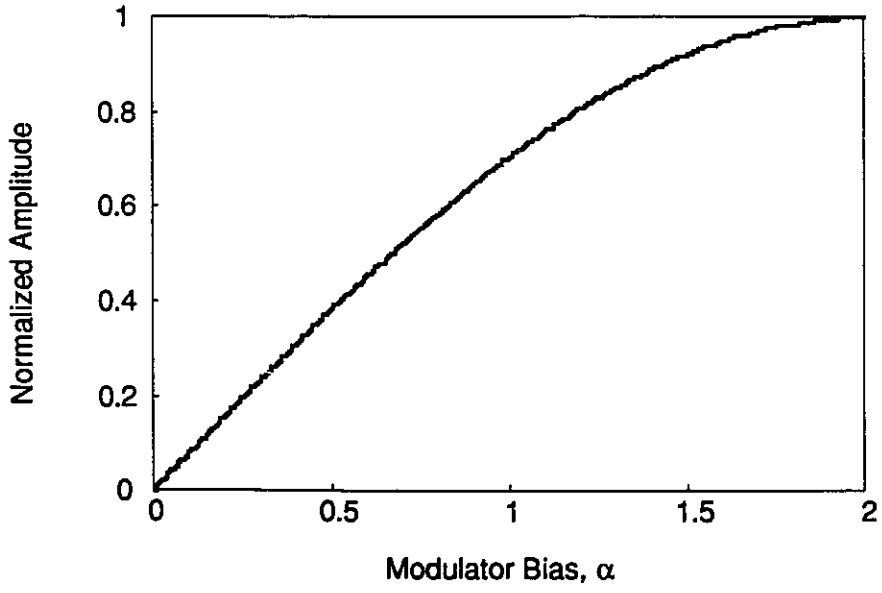

b) Voltage-Amplitude Curve.

Figure 3.7: Input-output characteristics of an external intensity modulator.

is

$$i_{k_I M}(t) = R\sqrt{P_{LO}P_m}m_{e_I}\cos\left(\frac{\alpha\pi}{4}\right)\cos[2\pi(f_{IF}-f_k)t - x_k(t) + \theta(t)]. \tag{3.33}$$

There is an additional problem in the case of OIM; the effective AM index is restricted by distortion considerations, due to the non-linearities at the extreme ends of the intensity modulator characteristic. Thus, for a proper intensity modulation, we should have (from (3.28) and (3.30))

$$|m_{e_I}y(t)| \leq \frac{\alpha\pi}{4}, \tag{3.34}$$

where $y(t)$ is as defined in (3.27). For an orthogonal set of signals, we note that we must have

$$|y(t)| \leq \sqrt{N}, \tag{3.35}$$

where N is the number of channels. After a substitution in (3.34), we find that

$$m_{e_I} \leq \frac{\alpha\pi}{4\sqrt{N}}. \tag{3.36}$$

The CNR is then

$$\text{CNR} = \frac{\frac{R^2}{2}P_{LO}P_m\cos^2(\frac{\alpha\pi}{4})m_{eI}^2}{\sigma_{sh}^2+\sigma_{th}^2+\sigma_{2d}^2+\sigma_{3d}^2+\sigma_{ct}^2}. \tag{3.37}$$

The second and third-order distortion terms are derived in Appendix B. We have proved the following expressions for the IMD_2 and IMD_3 powers:

$$\sigma_{2d}^2 = \frac{1}{8}R^2P_{LO}P_m h_2(\Delta\nu)P_2(k)\sin^2\left(\frac{\alpha\pi}{4}\right)m_{eI}^4 \tag{3.38}$$

and

$$\sigma_{3d}^2 = \frac{1}{32}R^2P_{LO}P_m h_3(\Delta\nu)P_3(k)\cos^2\left(\frac{\alpha\pi}{4}\right)m_{eI}^6. \tag{3.39}$$

The remaining noise terms are as defined below equation (3.17). By solving (3.37) for P_m, we get

$$P_m(\Delta\nu) = \frac{\sigma_{sh}^2+\sigma_{th}^2}{R^2P_{LO}\left[\frac{\cos^2(\frac{\alpha\pi}{4})}{2CNR}m_{eI}^2 - \frac{h_2(\Delta\nu)P_2(k)\sin^2(\frac{\alpha\pi}{4})}{8}m_{eI}^4 - \frac{h_3(\Delta\nu)P_3(k)\cos^2(\frac{\alpha\pi}{4})}{32}m_{eI}^6\right]}. \tag{3.40}$$

To maximize the receiver sensitivity, or minimize P_m, the optimum pair of parameters (α, m_{eI}) can be found. This has been done numerically, taking into account the

constraint stated in (3.36). The optimization is complicated here due to the fact that the theoretical $m_{eI_{opt}}$ is sometimes less than and sometimes greater than the practical limit (3.36), depending on the value of the coefficient α. Thus, in some cases suboptimum values have been chosen.

Fig. 3.8 shows the variations of the receiver sensitivity P_m versus α (3.40), for some values of the laser linewidth and for the worst channel (channel No. 1). Fig. 3.9 and Fig. 3.10 illustrate the optimum external modulator bias coefficient α_{opt}, and the corresponding optimum modulation index $m_{eI_{opt}}$ (values optimizing (3.40)), respectively as functions of the laser linewidth, for both the best and worst channels (channels No. 11 and No. 1, respectively). The previous results have been obtained for the multi-octave mode of operation. The same procedure has been followed in single-octave operation. For negligible laser linewidths, the results are consistent with [31].

The receiver sensitivity penalty due to phase noise is defined as in (3.25):

$$\Delta P_m(\text{in dB}) = 10\log\frac{[P_{m_{opt}}(\Delta\nu)]}{[P_{m_{opt}}(\Delta\nu = 0)]}. \tag{3.41}$$

3.3.4 Comparative Analysis of Performance

Fig. 3.11 shows the maximum receiver sensitivity for the OPM (3.24) and the OIM (numerical optimization of (3.40)) networks as a function of the laser linewidth and for the multi-octave mode of operation. The sensitivity for the OIM system lies between the best and worst channels for OPM. Furthermore, the channels are much closer in OIM than they are in OPM for any value of the laser linewidth; that is the overall performance of the OIM network, determined by the worst channel, will be better with respect to the laser phase noise.

The receiver sensitivity penalty due to phase noise, (3.25) and (3.41), is shown in Fig. 3.12; it is clear that the OIM scheme is more tolerant to laser phase noise than the OPM scheme. Finally, if we can tolerate up to 1dB penalty in the receiver sensitivity, we can read from Fig. 3.12 that the maximum allowable FWHM normalized linewidth $\Delta\nu_{max}/B$ is 4.5% for the OPM network and 5.7% for the OIM network. As an example,

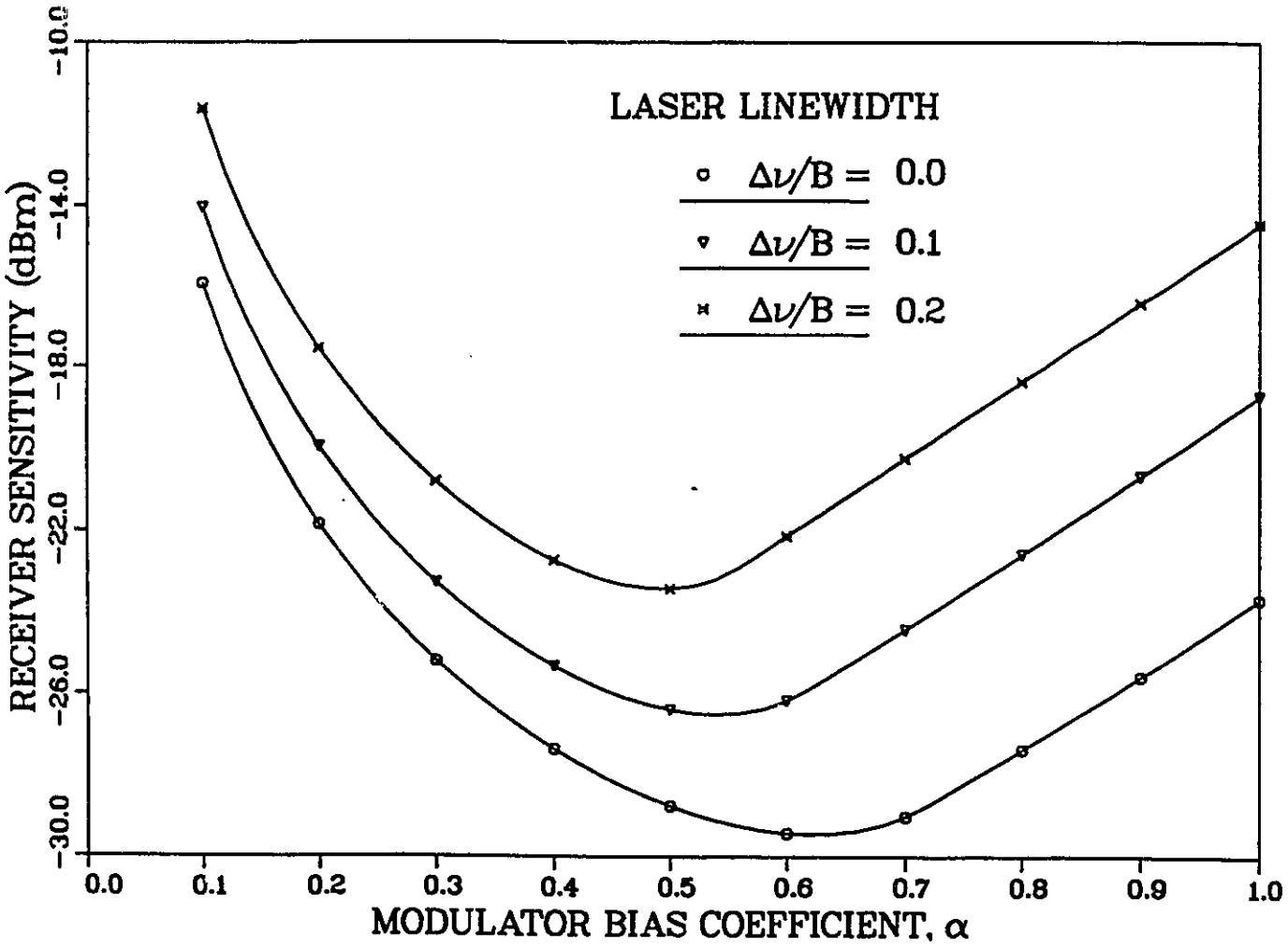

Figure 3.8: Worst channel sensitivity as a function of the external intensity modulator bias coefficient α in multi-octave operation and for N=20.

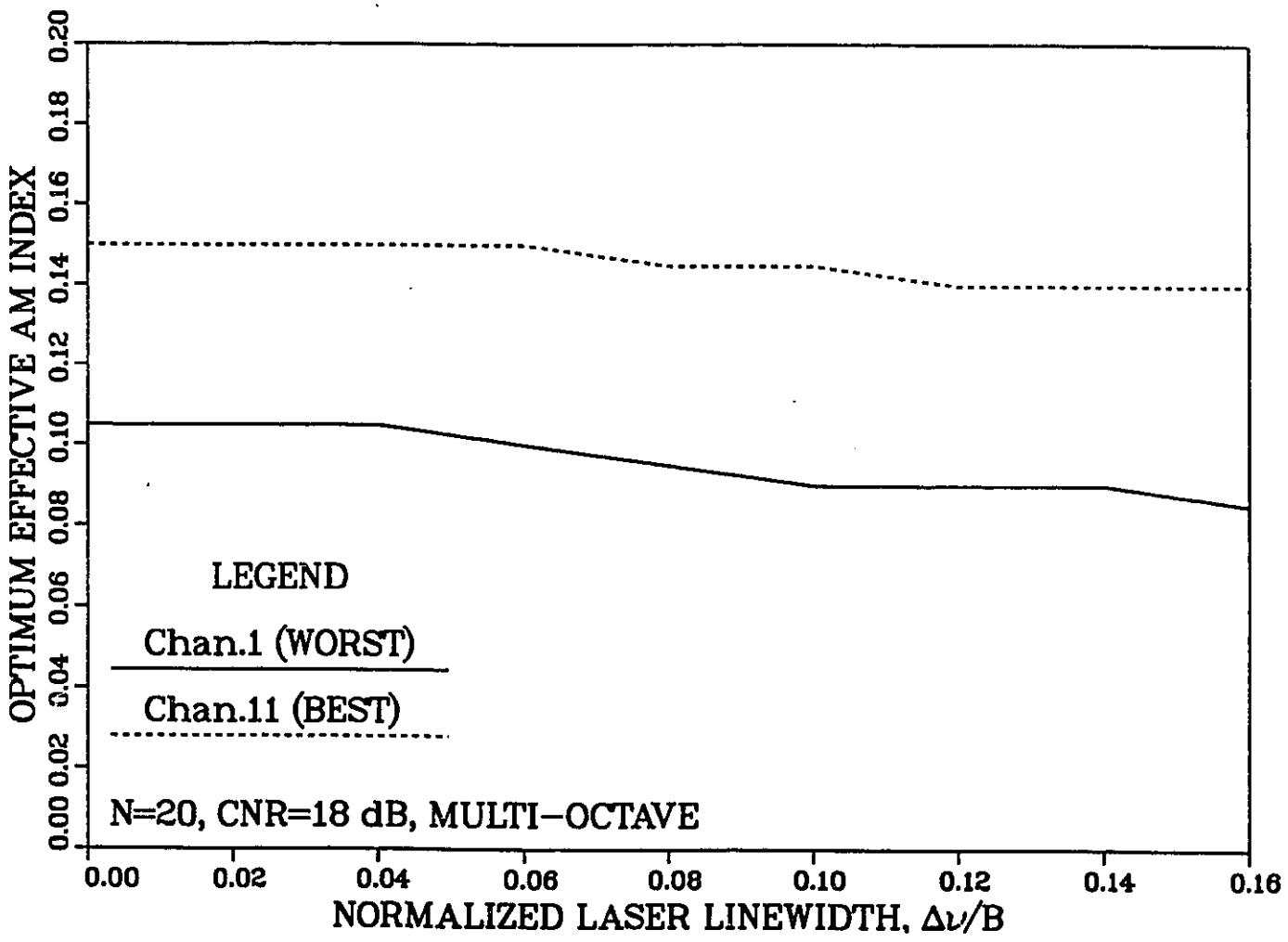

Figure 3.9: Optimal OIM index m_{ef} versus laser linewidth for the best and worst channels. Multi-octave operation, N=20.

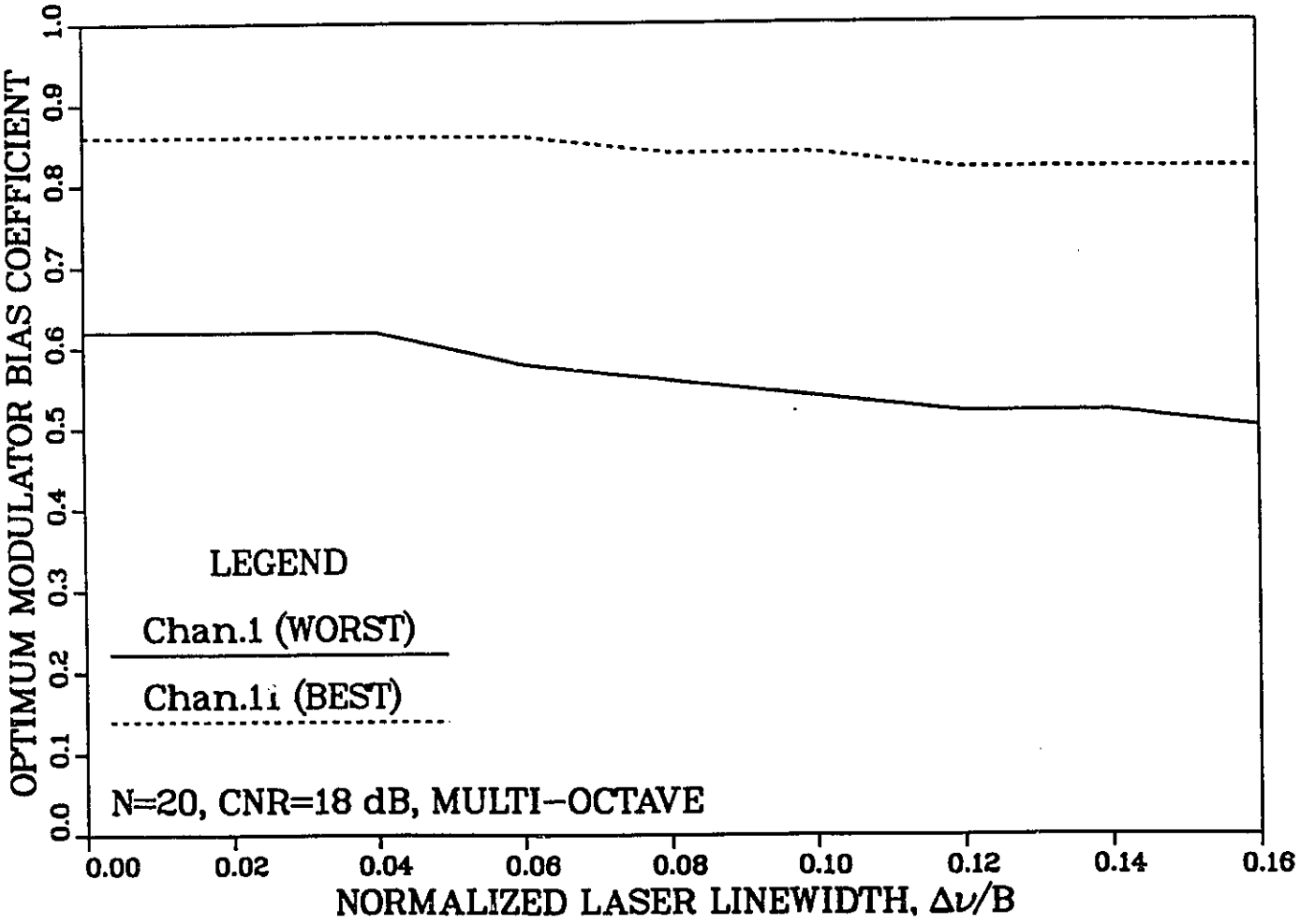

Figure 3.10: Optimal external intensity modulator bias coefficient α_{opt} as a function of the laser linewidth for the best and worst channels in multi-octave operation.

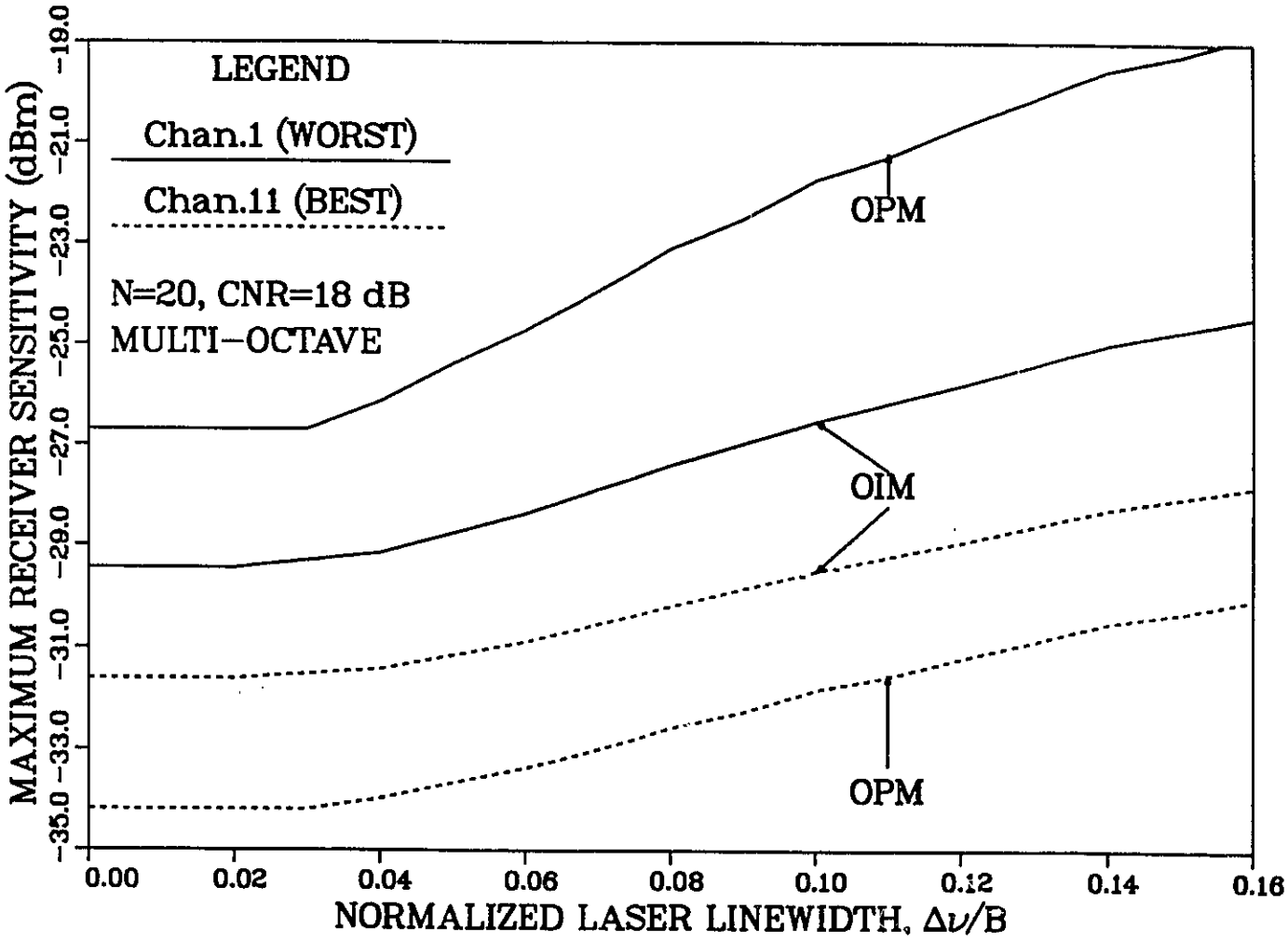

Figure 3.11: Comparison between the variations of the OIM and OPM maximum receiver sensitivity with respect to the laser linewidth. Multi-octave operation, N=20.

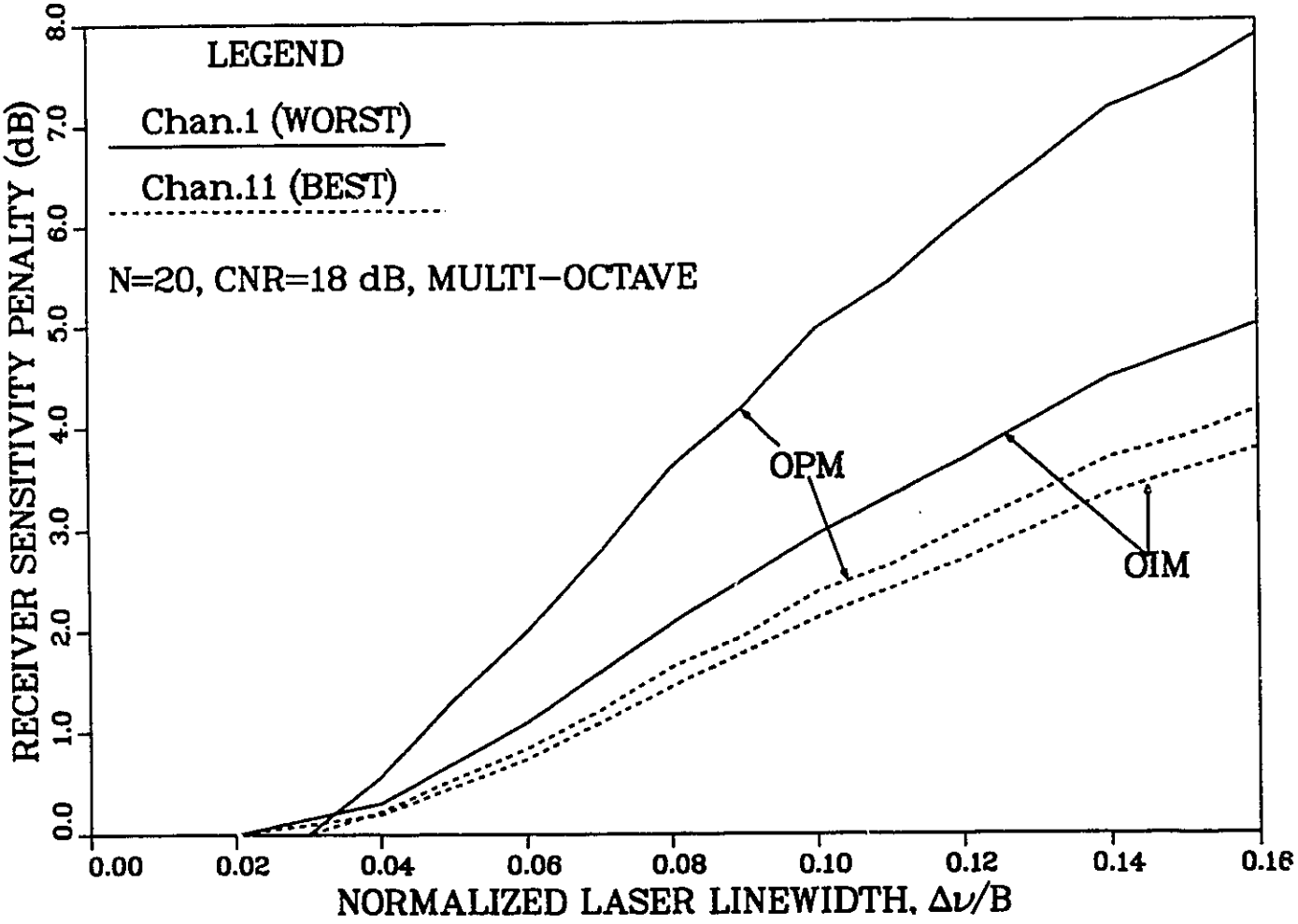

Figure 3.12: Receiver sensitivity penalty due to laser phase noise for OIM and OPM in multi-octave operation.

and for the data listed in Table 3.1, $\Delta\nu_{max} \approx 5.4$ MHz for OPM and $\Delta\nu_{max} \approx 6.8$ MHz for OIM.

In a single-octave mode of operation, only third-order intermodulation distortion IMD_3 affects the system; the best and the worst channels become then channels 1 and 11, respectively. The maximum receiver sensitivity and the corresponding penalty for both the OIM and OPM schemes are illustrated respectively in Fig. 3.13 and Fig. 3.14.

We can see that the best and worst channels are much closer than in MO mode of operation. The penalties due to phase noise in OPM and OIM are the same within 0.5 dB. However, the OPM scheme performs better in terms of the maximum receiver sensitivity as shown in Fig. 3.13. The limitations on laser linewidth are 6.2% and 6.5% for OPM and OIM respectively.

We have run the simulation for larger numbers of channels and the previous conclusions on the network performance remain valid. We note however that the modulation depth in OIM is severely restricted for large values of N, because of the constraint stated in (3.36).

3.4 Laser Phase Noise and the SCM/CD Multiple-Access Network

In the multiple-access network architecture (see Fig. 2.3), an exclusive subcarrier is assigned to each transmitter. There is no intermodulation distortion since the channels are not physically combined; there will be only harmonics created by the non-linear optical modulation of a single channel per transmitter. Since the amplitude of the harmonics is less than the amplitude of the IMD terms and their number being much smaller, the problem of nonlinearity is less severe than in the SCM/CD distribution network.

In order to extend our analysis to the SCM/CD multiple-access network, some assumptions must be made. First, we assume that all users transmit with the same average optical power and that the optical path loss is the same between any two users [5].

It has been noted in Section 2.1.2 that the main source of shot noise was the local

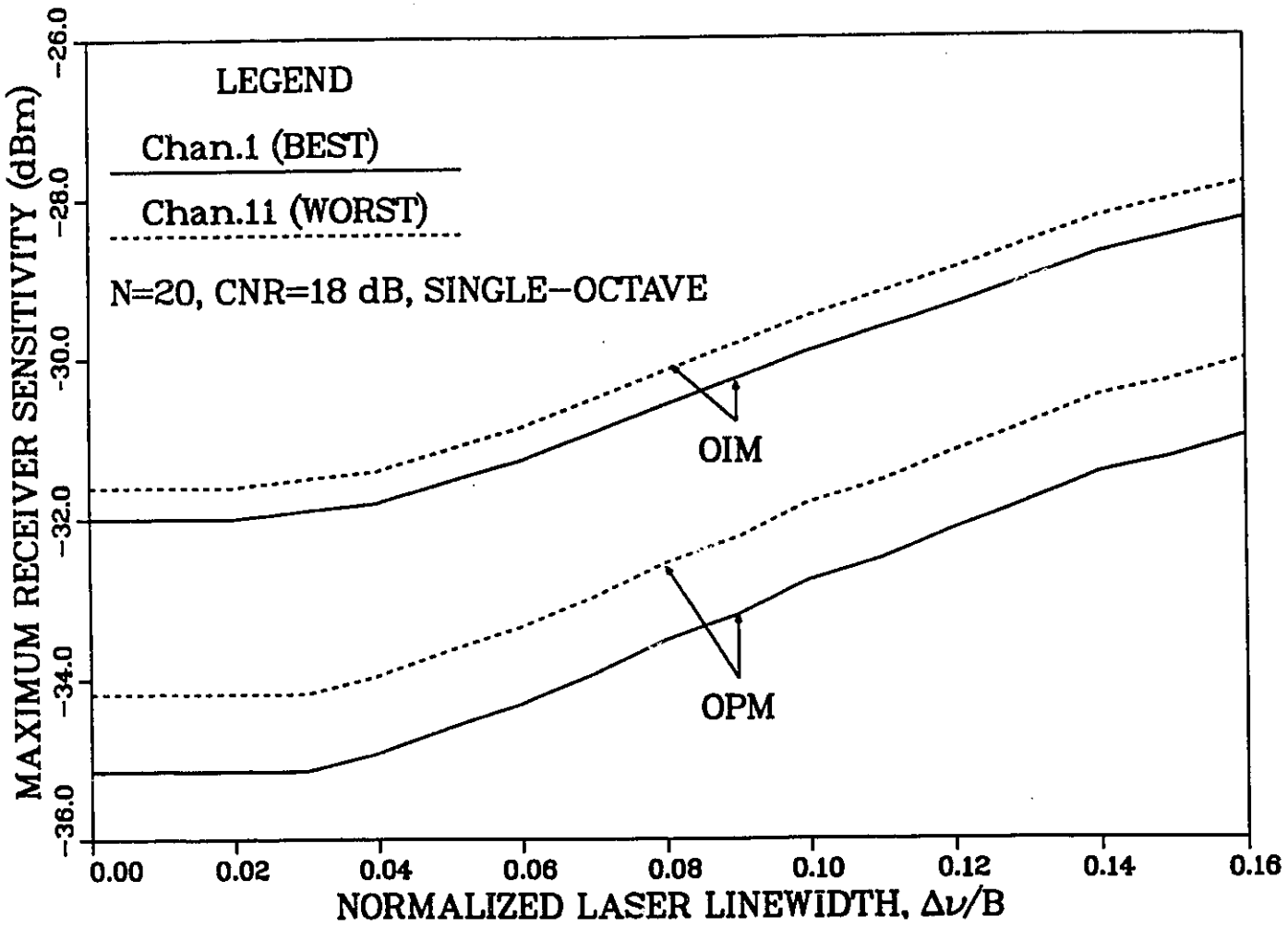

Figure 3.13: Comparison of the effect of laser phase noise on the maximum receiver sensitivity for the OIM and OPM in single-octave operation.

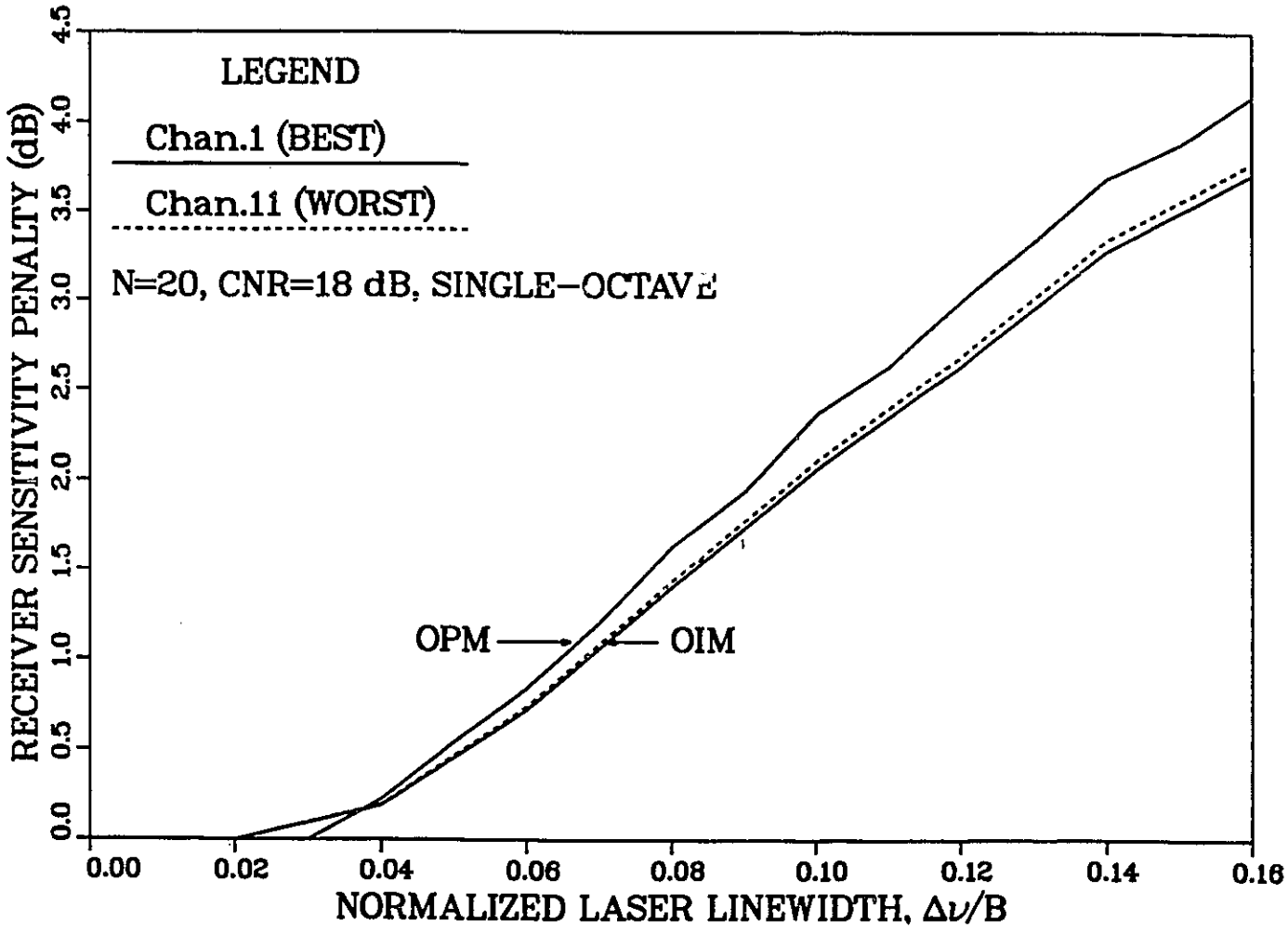

Figure 3.14: Receiver sensitivity penalty due to the laser phase noise for OIM and OPM. Single-octave operation, N=20.

laser oscillator, and that the excess shot noise produced by all the network users will remain small as long as the local oscillator power is much stronger than that of the received signal. A rather conservative estimate will be made in our analysis for simplicity purposes; we will assume that the excess shot noise power at the receiver is half of that due to the local laser oscillator.

3.4.1 Multi-Octave Operation

The same subcarrier frequency allocation as in the SCM/CD distribution network will be adopted here. This will ensure that the second-order harmonics will fall in the guardband between the channels. The maximum number of second-order harmonics will be two; this is for the worst channel (channel 1). The third-harmonic interference will be neglected.

Because the number of interferers is small in the second-order distortion noise, the assumption of a Gaussian distribution is not accurate. However, a frequency-domain analysis based on Gaussian approximation gives reasonably good estimates and leads to simple expressions [37].

In the case of OPM, and from (3.14), where N is set to 1, the power of the signal in the kth channel is given by

$$< i^2_{k_{PM}} >= 2R^2 P_{LO} P_s J_1^2(\beta), \tag{3.42}$$

and the power of the second-order harmonics affecting channel k is

$$< \sigma^2_{2h_{PM}} >= 2R^2 P_{LO} P_s h_2(\Delta\nu) P_2(k) J_2^2(\beta), \tag{3.43}$$

where $P_2(k)$=2 for the worst channel, and $h_2(\Delta\nu)$ is as given in (3.18). The expression for the receiver sensitivity (3.20) becomes then

$$P_s(\Delta\nu) = \frac{[\sigma^2_{sh} + \sigma^2_{th}]}{2R^2 P_{LO}\left[\frac{J_1^2(\beta)}{CNR} - h_2(\Delta\nu) P_2(k) J_2^2(\beta)\right]}, \tag{3.44}$$

where the shot noise power has been adjusted as explained in Section 3.4.

When OIM is used, the power of the signal in the kth channel is given by (B.3) in Appendix B:

$$< i^2_{k_{IM}} >= \frac{1}{2} R^2 P_{LO} P_m \cos^2\left(\frac{\alpha\pi}{4}\right) m^2_{e_I}. \tag{3.45}$$

From (B.6), the power of the second-harmonic interference affecting channel k is

$$< \sigma^2_{2h_{IM}} >= \frac{1}{32} R^2 P_{LO} P_m h_2(\Delta\nu) P_2(k) \sin^2\left(\frac{\alpha\pi}{4}\right) m^4_{e_I}, \tag{3.46}$$

and from (3.40), the receiver sensitivity is as follows:

$$P_m(\Delta\nu) = \frac{\sigma^2_{sh} + \sigma^2_{th}}{R^2 P_{LO}\left[\frac{\cos^2(\frac{\alpha\pi}{4})}{2CNR} m^2_{eI} - \frac{h_2(\Delta\nu) P_2(k) \sin^2(\frac{\alpha\pi}{4})}{32} m^4_{eI}\right]}, \tag{3.47}$$

where again $P_2(k) = 2$ for the worst channel.

The same method for finding the optimum modulation parameters for OPM and OIM is used once again. Fig. 3.15 shows the optimum phase modulation index β_{opt} for OPM (optimization of (3.44)), the optimum effective AM index $m_{e_{I_{op}}}$ and the corresponding intensity modulator bias coefficient α_{op} for OIM (optimization of (3.47)). These values have been computed for the worst channel.

The maximum receiver sensitivity, (3.44) and (3.47), for these optimum values is shown in Fig. 3.16 as a function of the laser linewidth. The results of the comparison are here clearly in favor of the OIM. Furthermore, and as illustrated in Fig. 3.17, the OIM scheme suffers less penalty from the laser phase noise than the OPM scheme does, for any value of the laser linewidth. The same conclusion was derived in the case of the SCM/CD distribution network.

From Fig. 3.17, it can be found that for a 1 dB penalty in the receiver sensitivity, the maximum allowable FWHM normalized linewidth is $\Delta\nu_{max}/B = 4.7\%$ for OPM and $\Delta\nu_{max}/B = 6.0\%$ for OIM. This is about the same result as for the distribution network.

3.4.2 Single-Octave Operation

In the single-octave mode of operation, there is no second-order distortion falling in the bandwidth of operation; the only effect caused by the laser phase noise is directly due to the enlargement of the IF bandwidth, which allows more and more shot and thermal noise into the receiver as the laser linewidth increases. As a consequence of that, all the channels of the multiple-access network will perform the same way. Moreover, the

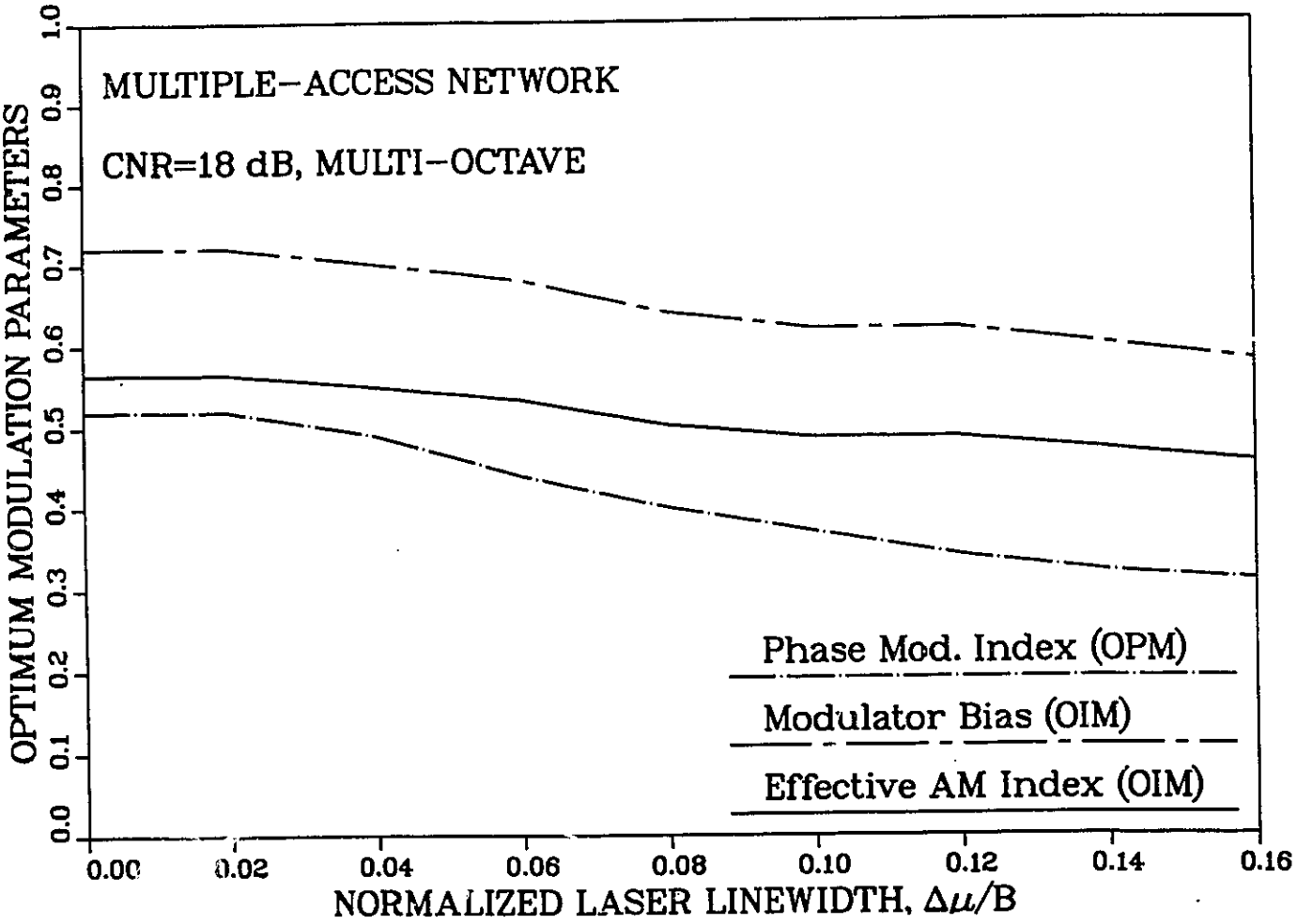

Figure 3.15: Optimum modulation parameters for OIM and OPM. Multiple-access network, multi-octave operation.

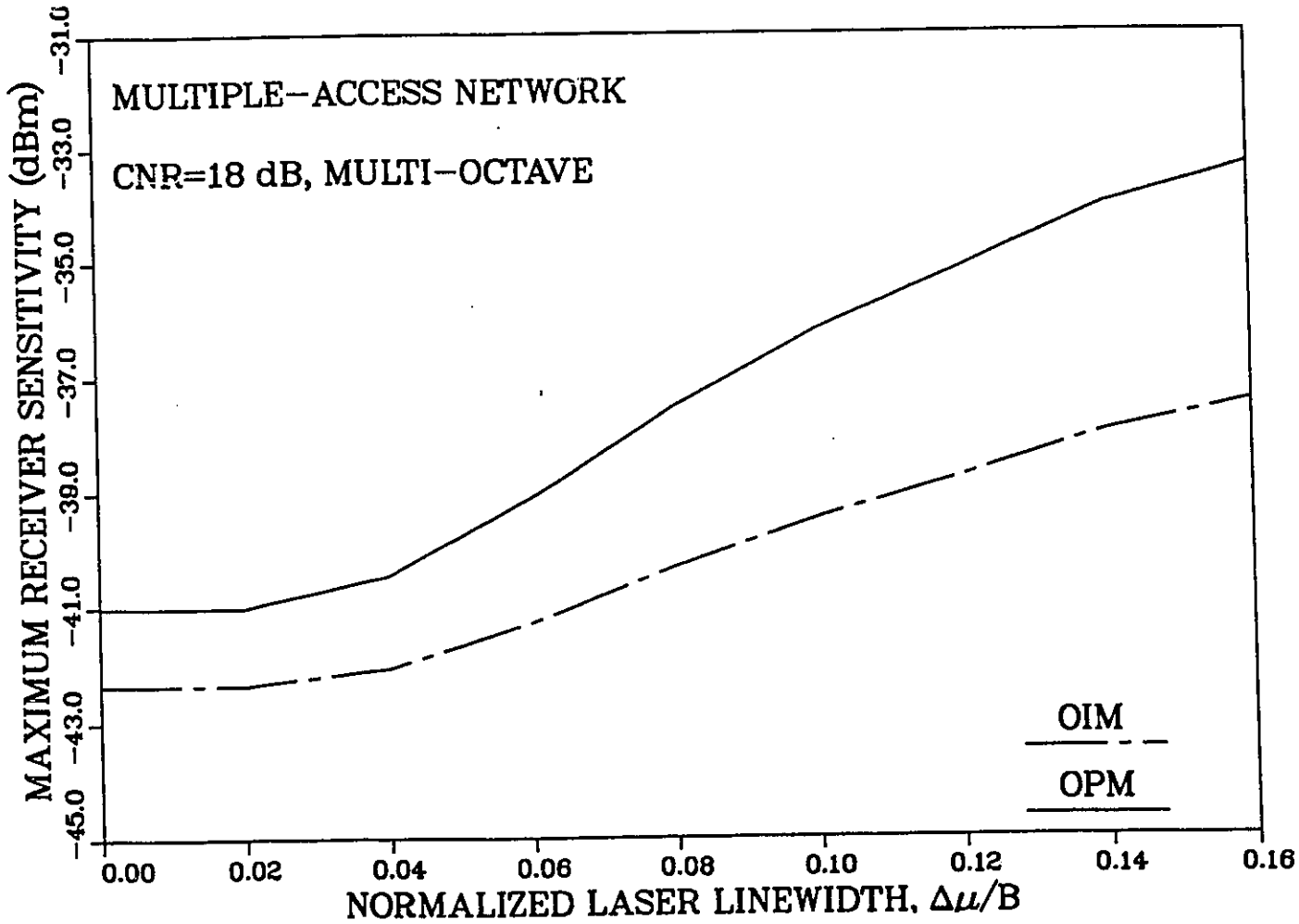

Figure 3.16: Comparison of the effect of the laser phase noise on the maximum receiver sensitivity for the OPM and OIM. Multiple-access network, multi-octave operation.

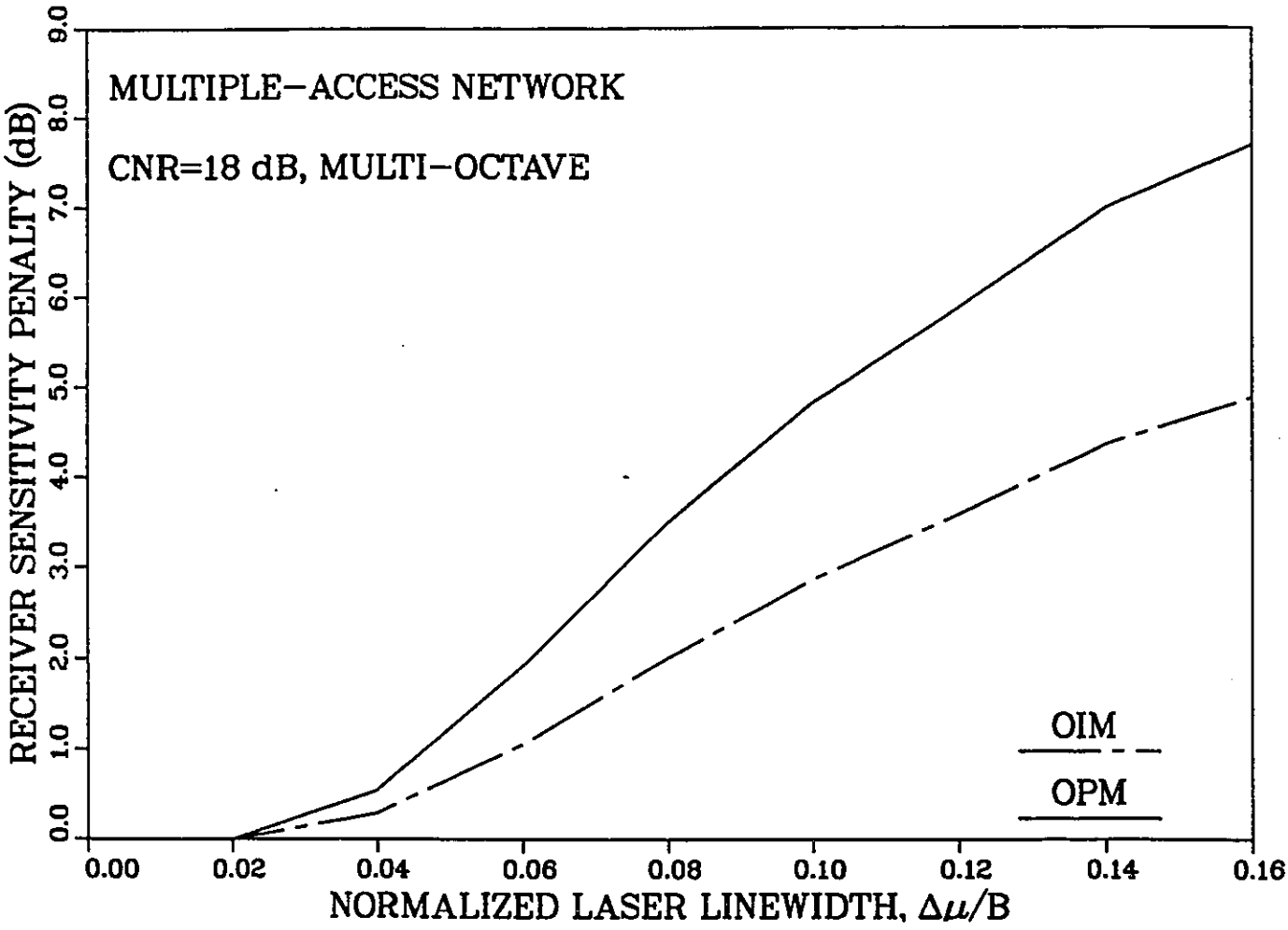

Figure 3.17: Receiver sensitivity penalty due to the laser phase noise for the multiple-access network and in multi-octave operation.

penalty due to the laser phase noise will not depend on the optical modulation technique used. Since the modulation index is not restricted by any nonlinearity considerations, the maximum receiver sensitivity is obtained for the maximum achievable effective optical AM index.

In the case of OPM, and from (3.42), the effective AM index is simply $J_1(\beta)$, and its maximum value is $J_1(\beta) = 0.58$ for $\beta \approx 1.8$. When OIM is used, the optimum modulation parameters are obtained from (3.45) in conjunction with (3.36). It is found that $\alpha_{opt} = 1.1$ and $m_{e_{opt}} = 0.86$. The maximum receiver sensitivity is illustrated in Fig. 3.18. This is a graphical interpretation of (3.44) and (3.47) where $P_2(k)$ is set to zero and where the above optimum values are used. As for the SCM/CD distribution network, OPM is by far the best suited modulation technique in the single-octave mode of operation.

Fig. 3.19 shows the penalty experienced by any channel of the multiple-access network. As expected, the same penalty is obtained for both OPM and OIM. For a 1dB penalty in the receiver sensitivity, the limitation on the laser linewidth is $\Delta\nu_{max}/B = 7.2\%$.

3.5 Number of Users

Another point of interest is the potential number of users for both the SCM/CD distribution network and the multiple-access network. The limitations on the receiver sensitivity set by the laser phase noise will in turn set limitations on the potential number of users of the network.

First, a distinction has to be made between the number of channels and the number of users, especially in the case of the multiple-access network. The potential number of users is mainly determined by the available power budget, whereas the number of channels is restricted by the available system bandwidth and the speed of the electronics used in the network. Thus if the number of users exceeds the number of channels in the multiple-access network, a protocol has to be used to resolve the contention for accessing the network.

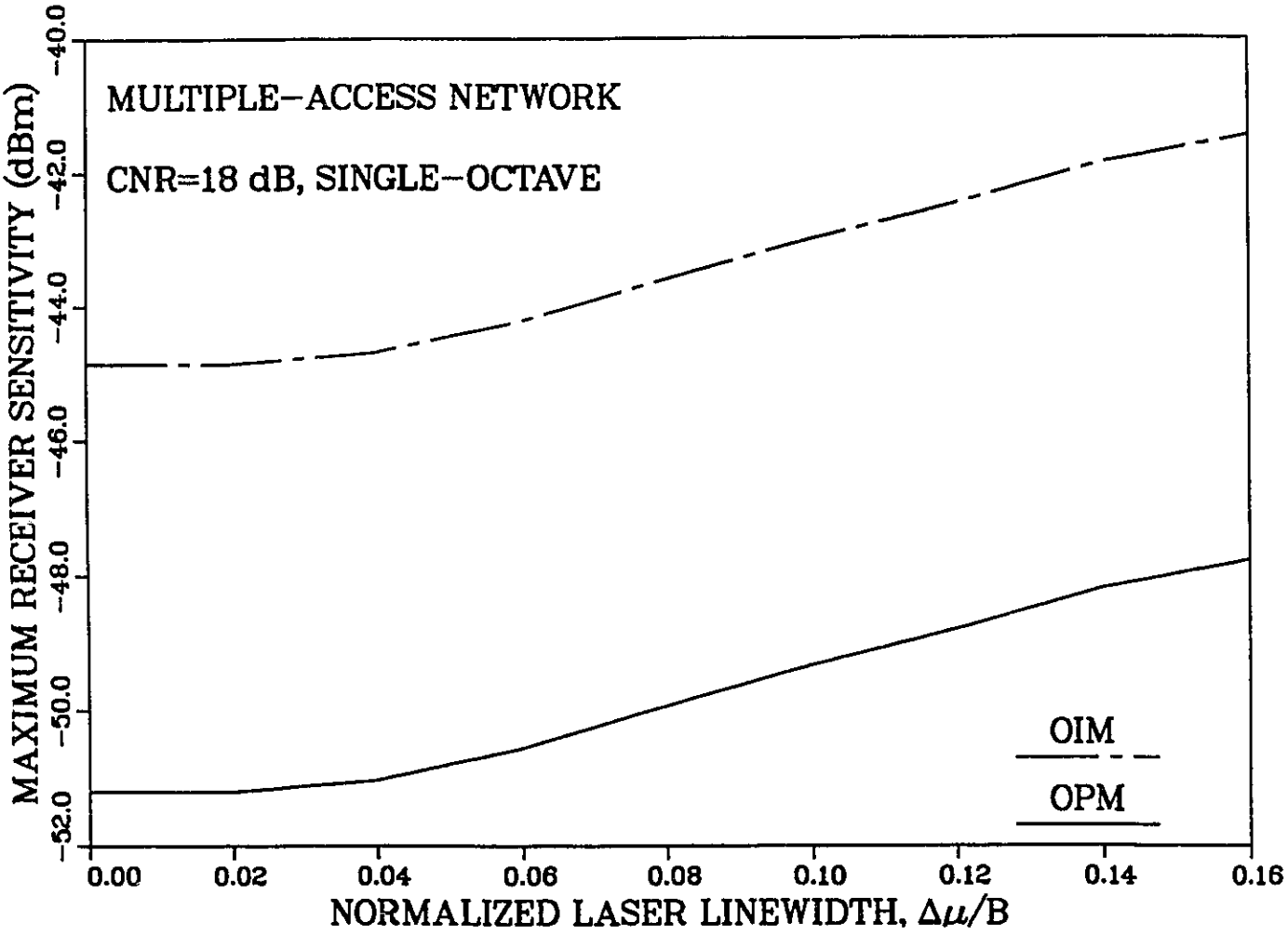

Figure 3.18: Comparison of the effect of the laser phase noise on the maximum receiver sensitivity for the OPM and OIM. Multiple-access network, single-octave operation.

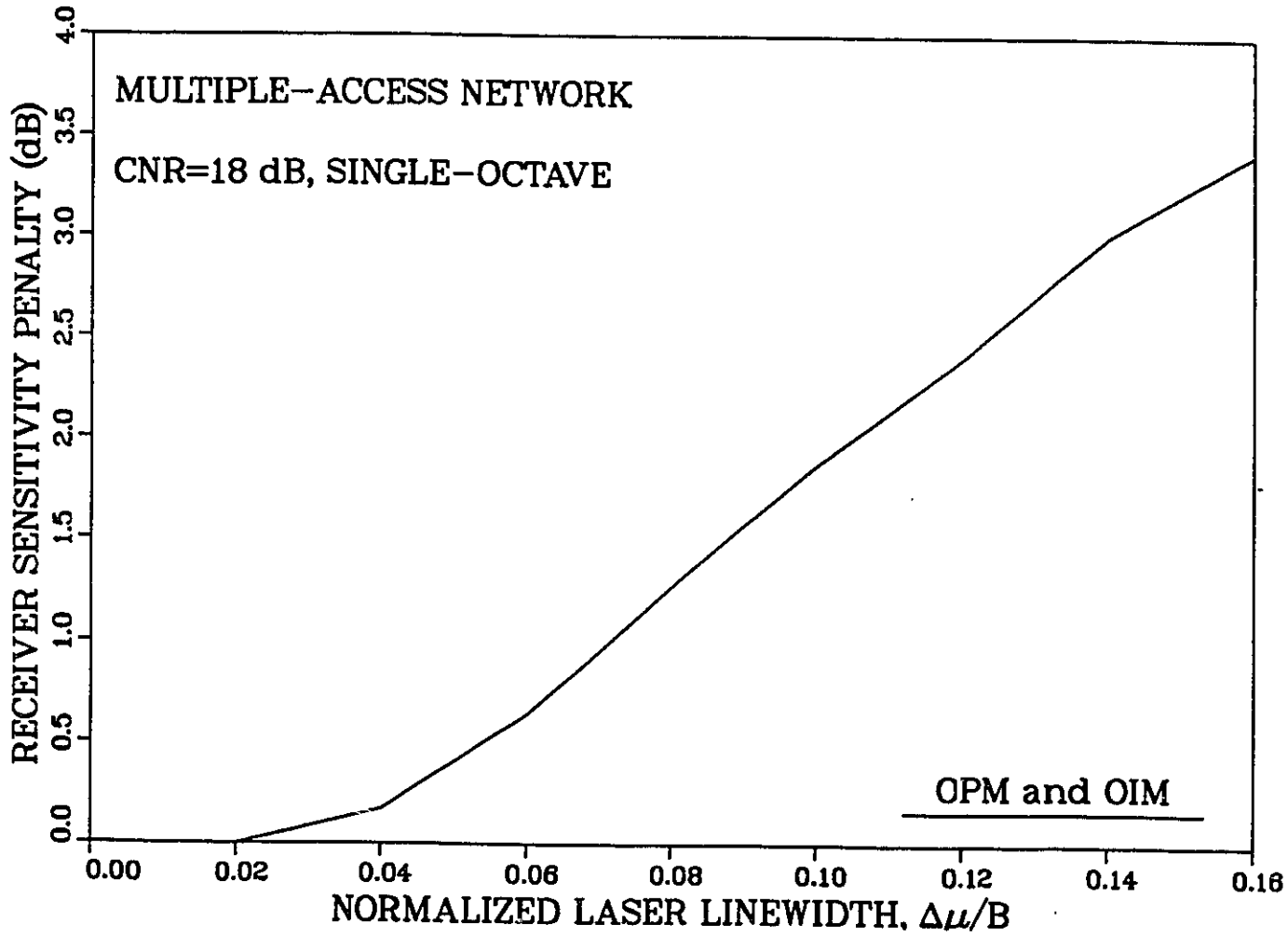

Figure 3.19: Receiver sensitivity penalty experienced by the channels of the multiple-access network in the single-octave mode of operation.

If an $M \times M$ star coupler, made of n stages of 2×2 (i.e., $M = 2^n$) is used, the maximum number of stages is given by

$$n_{max}[\Delta\nu] = \frac{P_t(dBm) - P_{opt}(\Delta\nu)(dBm) - l_f(dB)}{3 + l_c(dB)}, \tag{3.48}$$

where:

(i) P_t is the transmitter power of each user;

(ii) $P_{opt}(\Delta\nu)$ is the optimum receiver sensitivity. The expressions for $P_{s_{opt}}(\Delta\nu)$ in OPM and $P_{m_{opt}}(\Delta\nu)$ in OIM are used for each type of network and for the worst channel;

(iii) l_f is the fiber loss. We assume $l_f = 3$ dB, which corresponds to a fiber length of approximately 7.5 Km for a typical single-mode fiber having losses of 0.4 dB/Km; and

(iv) l_c is the coupler excess loss. It is assumed to be 0.1 dB.

The maximum number of users is then

$$2^{\lfloor n_{max} \rfloor} \leq M_{max} \leq 2^{\lfloor n_{max} \rfloor + 1}. \tag{3.49}$$

Fig. 3.20 and Fig. 3.21 show the maximum number of users for the distribution network and the multiple-access network, respectively. Since the potential number of users reflects the maximum receiver sensitivity for each case, it can be seen from Fig. 3.20 and Fig. 3.21 that, on the average, when comparing the performances for both multi-octave and single-octave modes of operation, the OIM modulation technique, when compared to OPM, allows for a significantly large number of users while it keeps a good performance with respect to the laser phase noise.

3.6 Summary

In this chapter, an investigation of the impact of laser phase noise on SCM/CD networks has been presented. Optical phase modulation (OPM) and optical intensity modulation (OIM) have been applied to two kinds of SCM/CD networks, namely the distribution network and the multiple-access network, and the optimized performances were compared. It was shown that, on the average, OIM has the potential for improved performance

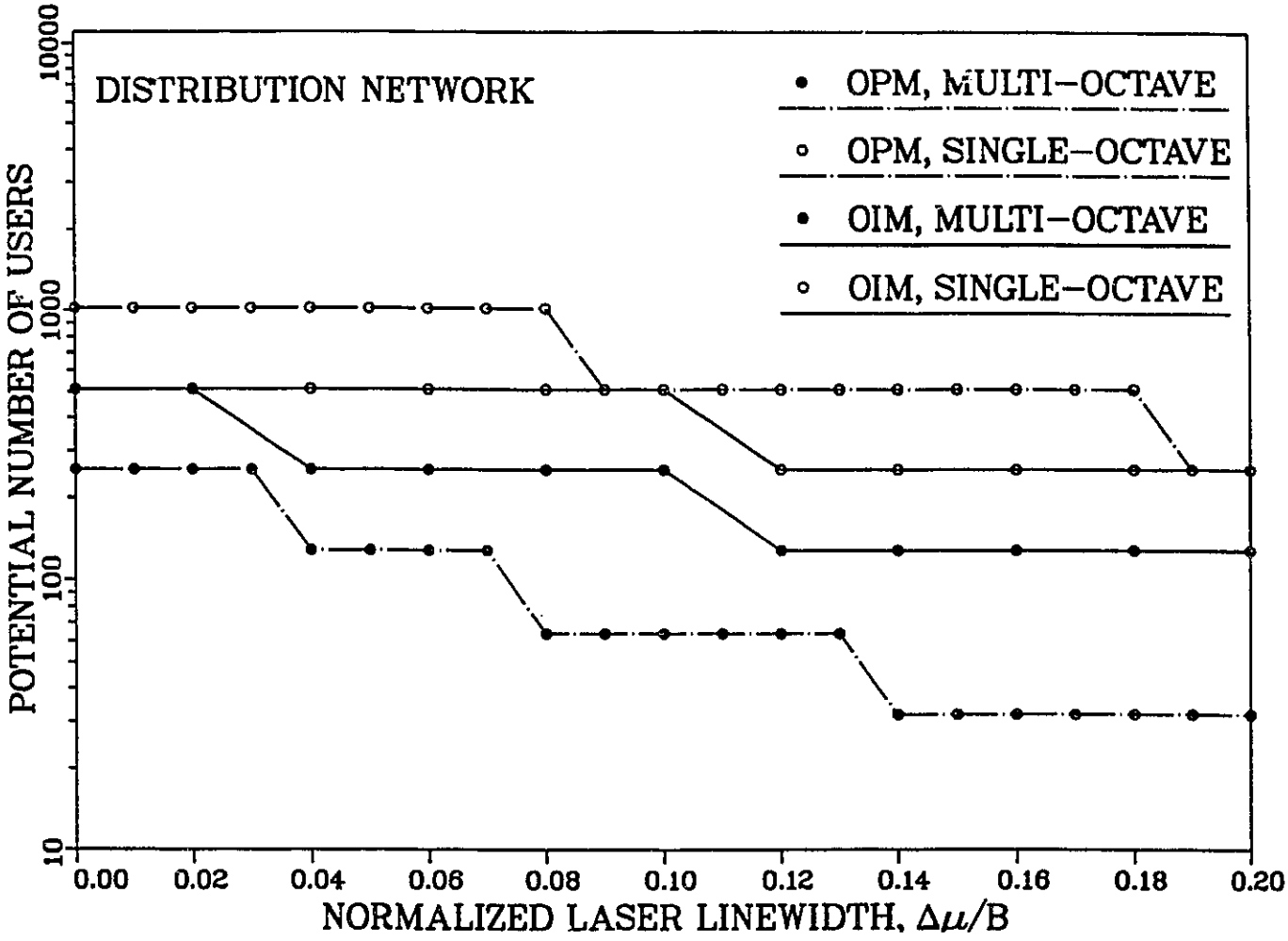

Figure 3.20: Potential number of users for the distribution network.

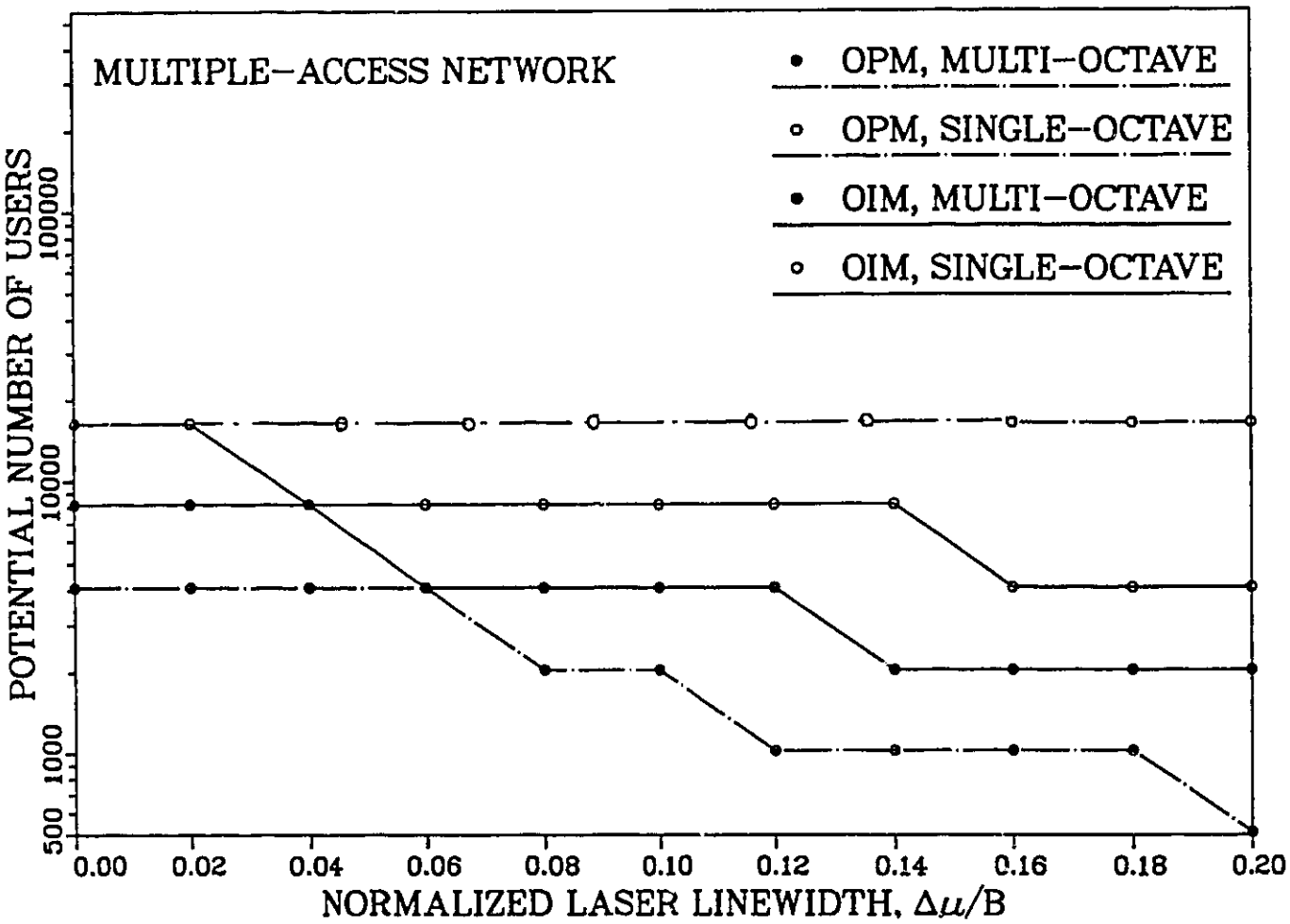

Figure 3.21: Maximum number of users for the multiple-access network.

compared to OPM; this is mainly due to the possibility of reducing the system nonlinearity by properly optimizing the modulator bias for each value of the laser linewidth.

The limitations on laser linewidth have been derived and it is clear that for bit-rates under about the 500 Mb/s range, the use of the presently available semiconductor lasers will lead to high penalties in the receiver sensitivity and will seriously degrade the performance of the networks. For bit-rates above that range, the SCM/CD networks prove to be competitive, and the use of semiconductor lasers does not affect seriously the systems performance.

The concept of SCM/CD networks can readily be extended to multiple optical wavelengths, thus making it compatible with the concept of optical FDM networks. It offers an efficient alternative for the implementation of photonic communication networks that can make use of the presently available technology.

Chapter 4

Phase Noise Cancellation Techniques

4.1 Introduction

It has been shown in Chapter 3 that for relatively low data transmission rates per channel, SCM/CD networks using semiconductor lasers would suffer severe phase noise induced degradation. The most obvious solution to alleviate the effect of the phase noise is to design semiconductor laser sources with narrow linewidths. Two successful approaches have been implemented. The first one consists of an injection locking of the semiconductor laser to a narrow-linewidth master oscillator laser (e.g., a gas laser) to reduce the linewidth to acceptable levels. While this technique can substantially reduce the linewidth, it is hardly justified to have a bulky gas laser at every network user location. A viable alternative is to use a centralized stable source, but this will make the problem of tunability difficult to be overcome.

The second technique makes use of an external cavity coupled to the semiconductor laser. The construction of such a laser is shown in Fig. 4.1. The principle of its operation is based on the reduction of the reflectivity of the semiconductor laser facets by providing anti-reflection coating. This will make the coupling between the semiconductor laser and the external resonator adequately strong and the oscillation frequency will

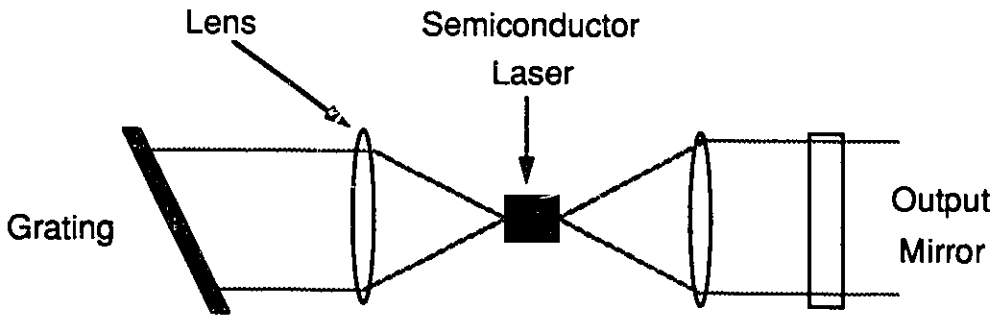

Figure 4.1: External-cavity semiconductor laser.

be determined predominantly by the external cavity resonance [41]. This technique can achieve narrow-linewidths down to several kiloHertz, but this is done at the expense of large-size cavities. It also requires precision mechanical alignments; all this makes the external cavity feedback laser a poor alternative to the simple monolithic device.

The complete solution to the problem of laser phase noise is to obtain and design the optimum receiver for a received signal contaminated by laser phase noise. This approach will be discussed in the next section. Other phase noise cancellation techniques will also be presented.

4.2 The Optimum Receiver

The detection problem of a signal contaminated by laser phase noise could be treated in the same fashion as it is done for conventional signal detection in communications. For instance, this problem can be viewed as finding the projections of the received signal on relevant signal directions. A diversity vector communication receiver will obtain the relevant received vector from the received waveform [42]. This is done by processing the received waveform in N separate branches of the receiver, where N is the number of relevant signal directions. In each branch, one projection of the relevant received vector is obtained. All the obtained projections will then be processed and a decision is made according to a decision rule. Thus for a received phase noisy signal in additive white

Gaussian noise, the signal decomposition into orthogonal set of vectors may be obtained by using the Karhunen-Loeve expansion. This approach has been investigated in [43]; it was found that the introduction of phase noise increases the number of relevant signal directions from a few to a very large number. This makes the task of designing an optimal receiver for signals corrupted by phase noise very difficult.

In Chapter 3, an ideal demodulator (see Fig.2.1 and Fig.2.3) was assumed. In practice, the demodulator will introduce a penalty on the performance of the receiver and further degradation is expected if asynchronous demodulation is used.

In [43], three binary modulation formats of the data, on-off keying (OOK), frequency shift keying (FSK) and differential phase shift keying (DPSK) were evaluated in terms of their bit-error performance in the presence of laser phase noise. Optimal detection strategies and suboptimal receivers were derived in each case. The analysis has shown, in particular, that asynchronous detection of binary FSK can be performed with an error probability penalty, due to phase noise, of less than 3 dB. This robustness against phase noise is attained by appropriately modifying the conventional envelope detector receiver. A wider front-end filter and an additional post-squaring filter were required. The modification of the conventional, optimal or suboptimal, receiver structure for binary modulation formats in order to make it less vulnerable to phase noise, is an important point in the analysis carried out in [43]. The author has emphasized the trade-off between the phase noise and the additive noise, since it is the combination of these noise processes that degrade the performance of the receiver.

4.3 Phase-Locking and Phase-Diversity Receivers

An alternative solution to the optimum receiver is to use, at the receiver, a phase-locked loop (PLL) that can partly track and thus reduce the effective phase noise, thus providing a reference signal that can be used to demodulate the received signal. If homodyne detection is used, there will be a need for an optical PLL, whereas in heterodyne detection, an electronic PLL at the IF stage is required. Simplified block diagrams of the PLL circuit

for both cases are shown in Fig. 4.2. However, it is very hard to design such kinds of PLL [44]. This is due to the fact that the bandwidth loop should be made wide enough to allow tracking of the phase noise variations, and at the same time narrow enough for a distortion-free demodulation. Thus, a careful optimization of the PLL bandwidth is required.

An interesting technique, called phase-diversity receivers, has been introduced to avoid the optical PLL in homodyne detection [30, 45, 46, 47]. The principle is shown in Fig. 4.3. The idea is similar to that of polarization-diversity receivers described in Section 2.2.3. An optical device called "a hybrid" combines the received signal and the local oscillator fields, E_s and E_{LO}, to produce a set of output fields $\{E_k\}$; the field E_k, in the kth branch of the receiver is a linear combination of E_s and E_{LO}. The fields $\{E_k\}$ are nonlinearly detected separately and the resulting currents $\{i_k\}$ are summed. The individual contributions of the phase noise towards the currents $\{i_k\}$ will cancel out and the resulting current will be independent of the phase noise.

For example, in the case of a two-branch ASK receiver, the hybrid will introduce a 90° relative shift between the signal and the local oscillator fields in one of the branches. Thus, we will have

$$\begin{aligned} E_1 &= L(E_s + E_{LO}), \\ E_2 &= L(E_s + jE_{LO}), \end{aligned} \tag{4.1}$$

where L is a constant of proportionality taking into account the losses introduced by the 90° hybrid. Assuming identical photodetectors and using (2.4) with $f_{IF} = 0$ (homodyne detection), the photocurrents in the two branches are given by

$$\begin{aligned} i_1 &= LR\sqrt{P_s P_{LO}}\cos[\Phi(t)], \\ i_2 &= LR\sqrt{P_s P_{LO}}\sin[\Phi(t)]. \end{aligned} \tag{4.2}$$

Thus, when the phase $\Phi(t)$, which includes the phase noise, varies, the currents i_1 and i_2 will not fade at the same time. If these currents are squared then summed together, the

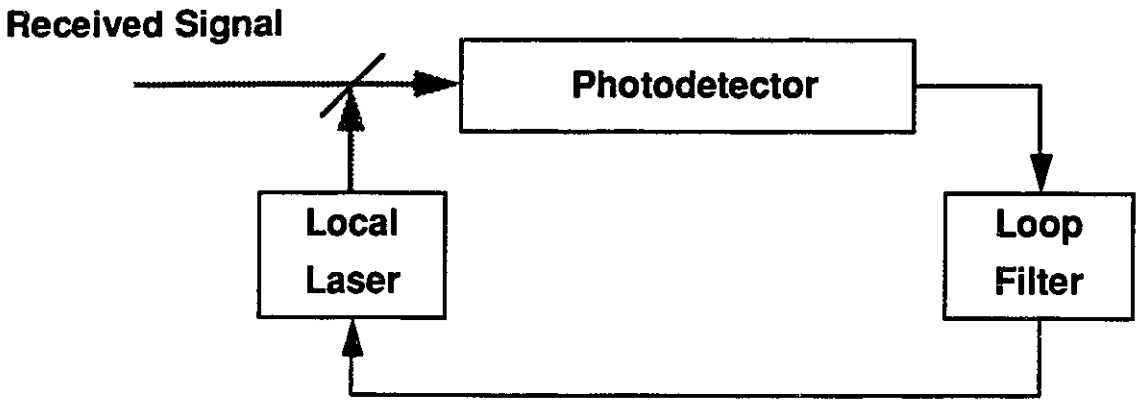

a) Optical PLL

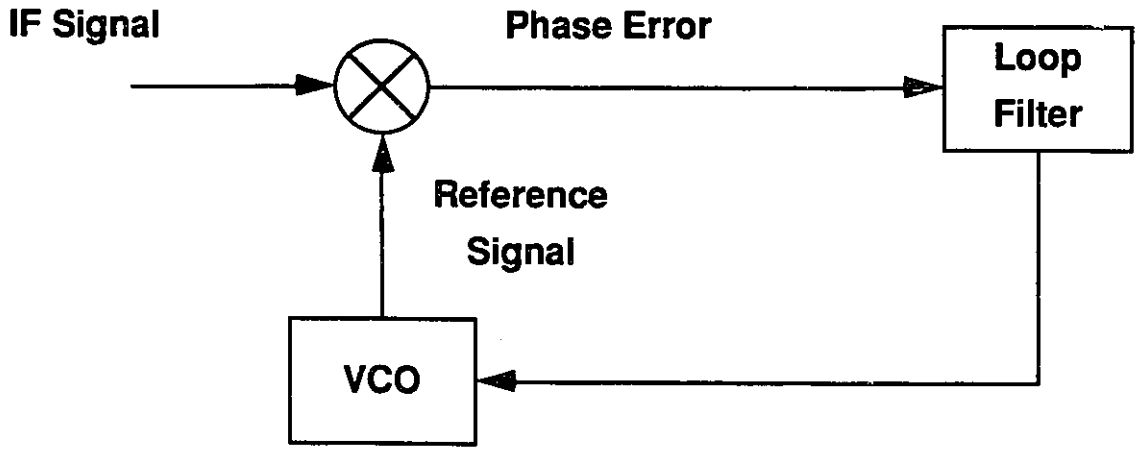

b) Electronic PLL

Figure 4.2: Principles of optical and electronic phase-locked loops.

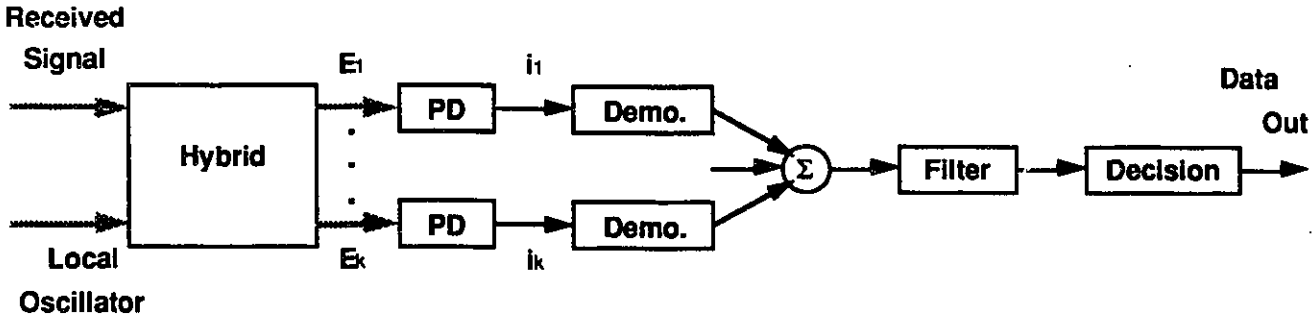

Figure 4.3: Phase-diversity receiver.

result is completely independent of the phase noise and is equal to

$$i_{TOT} = L^2 R^2 P_{LO} P_s. \tag{4.3}$$

The drawback of such a technique is that the number of electronic components is at least doubled. However this doubling of complexity is modest when compared to the needs of an optical PLL.

4.4 Transmitted Reference Signal

The problem of phase noise may be viewed as a lack of reference signal at the receiver. If the receiver is provided with a means to produce a reference signal, then the receiver output would not be affected by phase noise. The identical phase noise processes, in the transmitted and the reference signals, will cancel out to yield the pure modulated signal.

That is the essence of the transmitted reference techniques. The approach here is different from that of the previously presented methods in a sense that both the signalling mechanism and the receiver structure are optimized to achieve a good performance in the presence of the laser phase noise.

We can divide these techniques into three categories.

4.4.1 Direct Transmission of the Local Oscillator Signal

Here the local oscillator signal is transmitted in addition to the information signal. A beam splitter can be used to separate the output of the transmitter laser into two branches, one of which is modulated to generate the information signal and the other will serve as a reference signal at the receiver.

Ideally, the two signals would suffer the same amount of phase noise and the receiver would be able to carry a phase-noise free detection. However, because of the attenuation in the transmission channel, the reference signal at the detection would not be strong enough to be used as a local oscillator. The combined effects of the thermal noise and the dark current at the receiver would be significant and would overcome the effect of the laser phase noise that we intend to eliminate.

An optical amplifier can be used [48] to boost the local oscillator signal. The optical amplifier will introduce additive noise in both the information and reference signals.

More investigation should be carried out to evaluate the performance improvement introduced by the use of optical amplifiers.

4.4.2 Transmission of a Reference Signal

A different scheme is described here. A local oscillator laser is present at the receiver, and the purpose of these techniques is to provide the receiver with a reference signal that will be used after photodetection to undo the effect of the laser phase noise.

Since it is more convenient to transmit both the reference and the information signal through the same fiber, an orthogonality condition between the two signals should be provided to avoid interference. The receiver then extracts the signals from the sum signal.

Two methods have been reported to achieve the orthogonality condition [49]-[52]. The first one introduces a frequency shift between the two optical signals, i.e., the information and the reference signals. The frequency shift is appropriately chosen so that no spectral overlapping occurs; this means that the frequency shift should be much greater

than both the data rate and the laser linewidth.

In Fig. 4.4, the principle of this method is shown. The receiver can separate the two signals by the appropriate IF filtering.

The second method introduces an orthogonality in the polarizations of the two signals. An implementation example of this method is shown in Fig.4.5. A polarizing beam splitter separates the orthogonal polarizations x and y of the transmitter laser; one component is modulated with the information data, while the other will serve as a phase reference. The receiver can separate the two signals by using another polarizing beam splitter.

In both methods, the receiver at the IF stage gets two copies of the phase noisy IF carrier, one modulated and the other unmodulated. These two signals are then correlated, and through the mean of a nonlinear processing, the common phase noise term is cancelled.

These techniques reduce to some extent the effect of the laser phase noise, but a perfect phase noise cancellation is not possible due to the additive noise introduced in the photodetection process.

4.4.3 Miscellaneous Techniques

In this category, a brief description of some other phase noise cancellation circuits that have been suggested is presented. In [53] and [54], the authors propose two different schemes to extract a reference signal from the received signal by means of appropriate IF filtering. In Fig. 4.6, the circuit proposed in [53] is shown. One branch of the circuit will filter out the data channels , while the other will pass the IF carrier only. The two signals are correlated by the mean of an electrical mixer, and because the phase noise is common to both signals, it will effectively be cancelled.

For a complete cancellation, a perfect matching of the propagation times in the two branches should be realized, i.e., $\tau = 0$. This is however difficult to satisfy in practice.

There are other means to reduce the effect of laser phase noise. In [55] and [56], the authors propose nonlinear receivers. These are based on nonlinear postdetection processings such as those using delay-line discriminators and limiter-discriminator detectors.

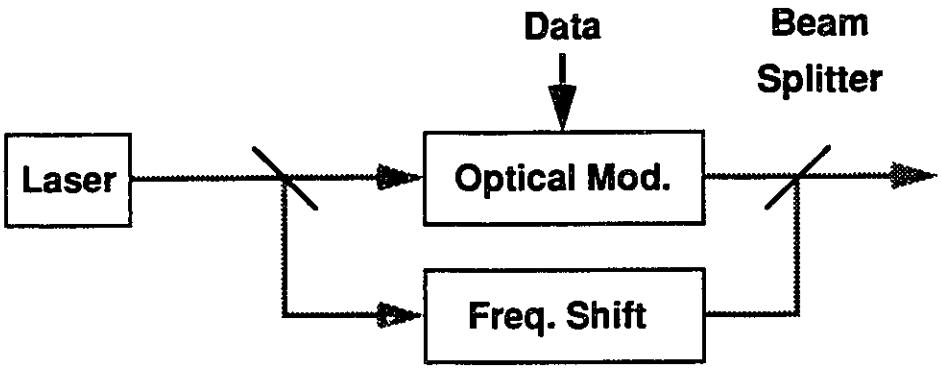

a) Transmitter Configuration

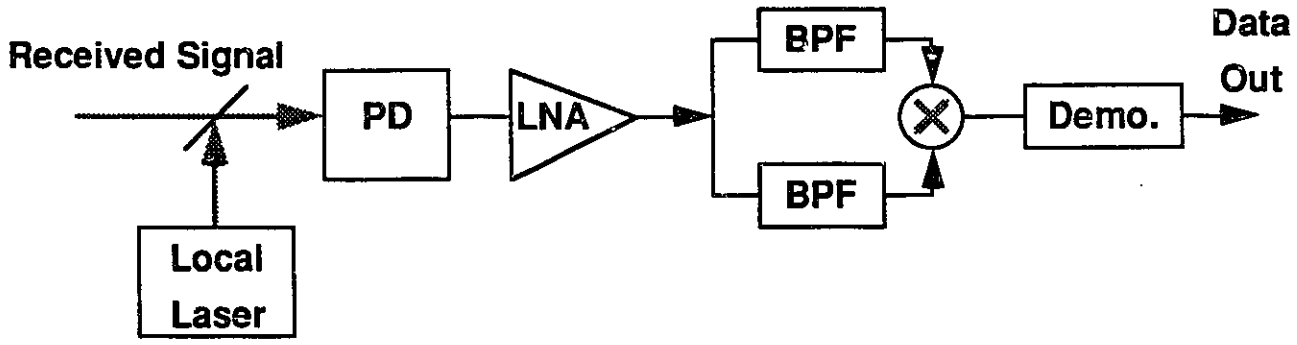

b) Receiver Configuration

Figure 4.4: Dual-frequency phase-noise-cancelling scheme.

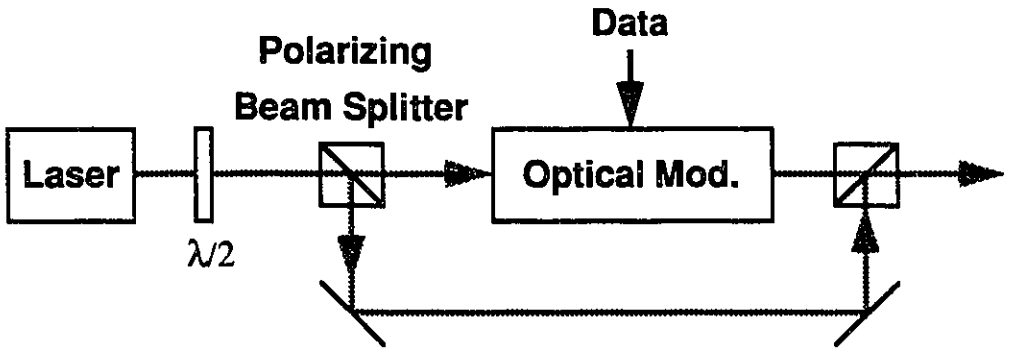

a) Transmitter Configuration

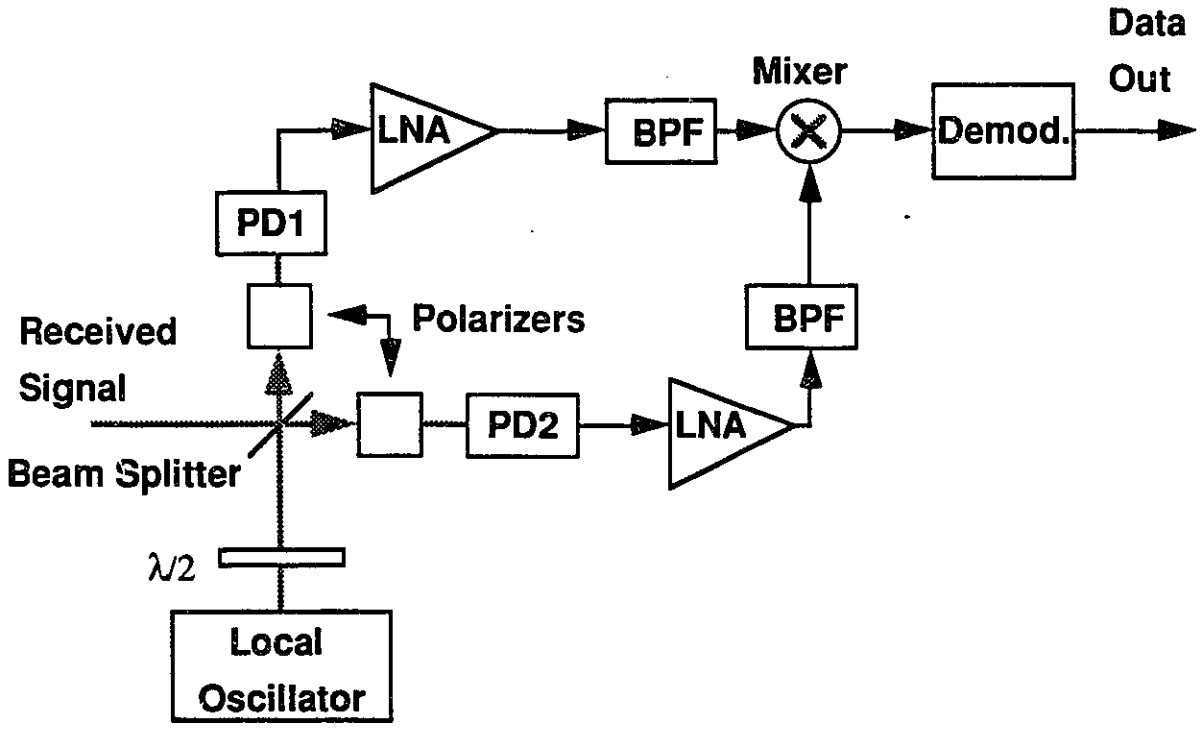

b) Receiver Configuration

Figure 4.5: Orthogonal-polarization phase-noise cancellation technique.

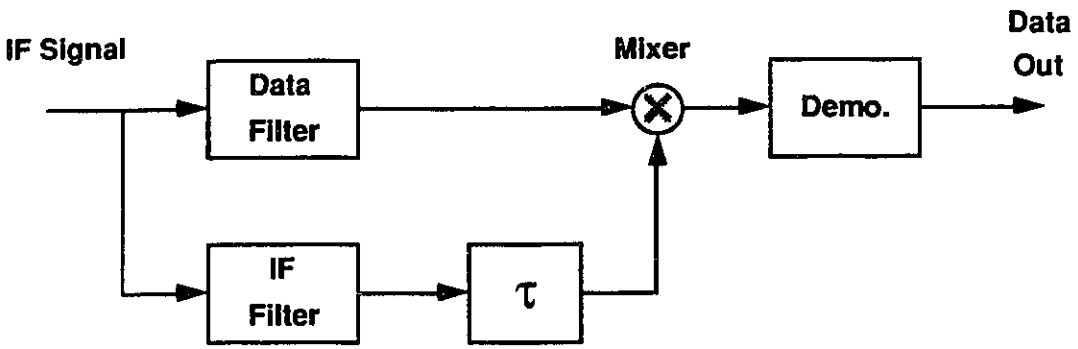

Figure 4.6: A phase noise cancellation circuit for an SCM system.

The analysis of these techniques is outside of the context of this thesis.

It should finally be noted that such methods are designed for specific modulation schemes (FSK, DPSK, ...etc) and some of these work only for a specific value of the modulation index, like the circuit presented in [56].

Chapter 5

Conclusions and Suggestions for Future Work

In this thesis, we have attempted to provide a study of the performance of subcarrier-multiplexed photonic networks in the presence of the laser phase noise. The subcarrier multiplexing at the microwave level, associated with coherent detection at the optical level, offers an efficient alternative for the implementation of photonic networks using the commercially available electronic and optical components. The emphasis of the investigation has been on the receiver sensitivity performance of two kinds of subcarrier-multiplexed photonic networks, where the transmitter and receiver lasers are corrupted by significant phase noise.

After the introduction, the concepts of multi-channel subcarrier-multiplexed photonic networks using coherent detection were presented in Chapter 2. Both the SCM/CD distribution network and the SCM/CD multiple-access network have been described. The operation of each network has been explained and the most important problems that eventually set limitations on the performance of such networks have been discussed. An explanation of the origins of the laser phase noise has been provided, as well as a description of the mathematical model that has been widely accepted for theoretical analyses.

In Chapter 3, the effect of laser phase noise on both kinds of SCM/CD networks has been investigated. A simple model has been used to describe the effect of phase noise on

the power spectrum of the received signal. Then, the performance of the SCM/CD networks for two optical modulation formats, namely the optical phase modulation (OPM) and the optical intensity modulation (OIM) has been optimized. The modulation parameters have been optimized for the best achievable receiver sensitivity in each case. It has been shown that for the SCM/CD distribution network, the OIM scheme outperforms the OPM scheme in terms of the tolerance to the laser phase noise, in a multi-octave operation. In a single-octave mode of operation, the OPM allows for higher receiver sensitivities while the effect of the laser phase noise for both modulation schemes is basically the same. The performance of the distribution network remains essentially the same when the number of channels increases. However, because of the non-linear distortion introduced by the external intensity modulator, the modulation depth in OIM is severely restricted as the number of channels becomes large.

In the case of the multiple-access network, the investigation has led to the same conclusions as for the distribution network, with the difference that the intermodulation distortion is less severe in this case; thus, the modulation depth in OIM can be set to higher values.

The limitations on laser linewidths have also been derived, and it has been shown that for relatively high bit-rates per channel, above half the gigabit per second, the SCM/CD network approach has proved to be competitive. For bit-rates under this level, the use of semiconductor lasers will seriously affect the performance of the networks.

A discussion on the potential number of users has also been provided and it was concluded that the OIM scheme offers, on the average, a better immunity to the laser phase noise while it allows for a significantly large number of users.

In Chapter 4, different techniques to reduce the effect of laser phase noise have been discussed. While the progress in opto-electronics and narrow-linewidth semiconductor lasers is the key to cost-effective photonic networks, various methods have been presented in the literature to overcome, or at least to reduce, the laser phase noise impact on coherent photonic systems. The discussion coverage ranges from the optimum receiver in the presence of phase noise to the transmitted reference signal techniques. Because of

the compatibility of the SCM network approach with the concept of FDM networks, and the possibility of using readily available microwave and optical components, the approach can constitute an excellent alternative, especially for the purpose of the distribution of services.

The major problem being the laser phase noise, many issues related to it need to be clarified before we can claim that phase noise will not be a significant issue in coherent optical networks. For example, future work on this topic could include the effect of the laser phase noise on the intermodulation distortion as well as on the cochannel interference. A clear understanding of the interaction between these three phenomena will help in improving the performance of the network receivers.

Another important issue is the derivation of the statistics of the variables, affected by phase noise, that are encountered in the performance analysis of communication systems. A compact statistical description of these random variables would reduce significantly the design complexity of optimum receivers in the presence of phase noise.

While this thesis has focused on coherent photonic networks, the subcarrier multiplexing approach can be implemented using direct detection. Such an approach might be very attractive in the near future as optical amplifiers, such as erbium-doped fiber amplifiers, are becoming available.

Although a direct detection receiver would not suffer from phase noise in a single channel configuration, in a multi-channel network however, the interfering signals will yield cross terms that contain the effect of phase noise. Furthermore, the optical noise introduced by the optical amplifier will also serve as an interference. In both cases, the interfering signals will play a role similar to that of a local oscillator laser in coherent detection. An investigation of the effect of phase noise on direct detection photonic networks must be carried out to predict the performance of such networks and find possible remedies.

Appendix A

Evaluation of the Filtering Coefficients for the Intermodulation Distortion

When a specific channel is selected at the receiver of the SCM/CD network, the bandpass filter will pass, along with the desired channel, a certain amount of second-order and third-order intermodulation distortion power.

To evaluate how much IMD's power gets through the bandpass filter, Olshansky and Gross [17] define a coefficient h that takes into account this; for the IMD_2, it is

$$h_2 = \frac{\int_{-\infty}^{+\infty} S_i(f) * S_j(f)|H_{BP}(f)|^2 df}{\int_{-\infty}^{+\infty} S_i(f) * S_j(f) df}, \tag{A.1}$$

and for the IMD_3 it is

$$h_3 = \frac{\int_{-\infty}^{+\infty} S_i(f) * S_j(f) * S_k(f)|H_{BP}(f)|^2 df}{\int_{-\infty}^{+\infty} S_i(f) * S_j(f) * S_k(f) df}, \tag{A.2}$$

where * denotes convolution, $S_i(f)$ is the power spectrum of the ith channel and $H_{BP}(f)$ is the frequency response of the bandpass filter. In order to evaluate these coefficients in the presence of the laser phase noise, we will assume, as in [32], that the phase noise does not influence very much the power spectrum of the IMD's so that the degradation of performance is mainly due to enlarging the bandwidth of the bandpass filter, which allows more IMD_2, IMD_3, thermal and shot noise into the receiver.

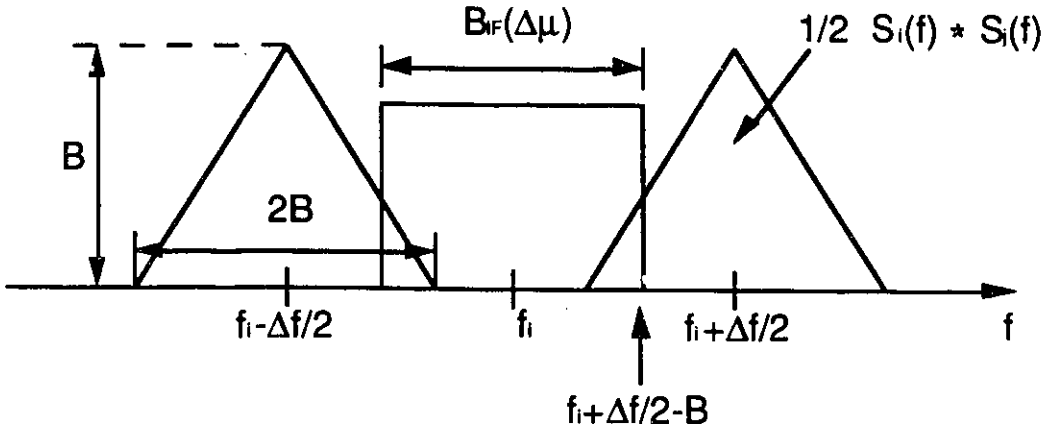

Figure A.1: Evaluation of the filtering coefficient for the IMD_2.

To simplify the calculations, we will assume an ideal bandpass filter frequency response centered at frequency f_0 with a bandwidth $B_{IF}(\Delta\nu)$, as defined in (3.10). That is:

$$H_{BP}(f,\Delta\nu) = \begin{cases} 1, & f_0 - \frac{B_{IF}(\Delta\nu)}{2} \le f \le f_0 + \frac{B_{IF}(\Delta\nu)}{2}; \\ 0, & \text{otherwise.} \end{cases} \tag{A.3}$$

The coefficients in (A.1) and (A.2) can be then rewritten as follows:

$$h_2(\Delta\nu) = \frac{\int_{-\infty}^{+\infty} S_i(f) * S_j(f)|H_{BP}(f,\Delta\nu)|^2 df}{\int_{-\infty}^{+\infty} S_i(f) * S_j(f) df}, \tag{A.4}$$

and

$$h_3(\Delta\nu) = \frac{\int_{-\infty}^{+\infty} S_i(f) * S_j(f) * S_k(f)|H_{BP}(f,\Delta\nu)|^2 df}{\int_{-\infty}^{+\infty} S_i(f) * S_j(f) * S_k(f) df}. \tag{A.5}$$

Note that, because of the assumption made on the power spectrum of the IMD's, the signal power spectrum that appears in the convolutions in both (A.4) and (A.5) is that of the signal in an uncontaminated channel, as defined in (3.8).

Fig. A.1 illustrates the different steps in evaluating $h_2(\Delta\nu)$. We first have

$$\int_{-\infty}^{+\infty} S_i(f) * S_j(f) df = 2\,[B]^2, \tag{A.6}$$

then

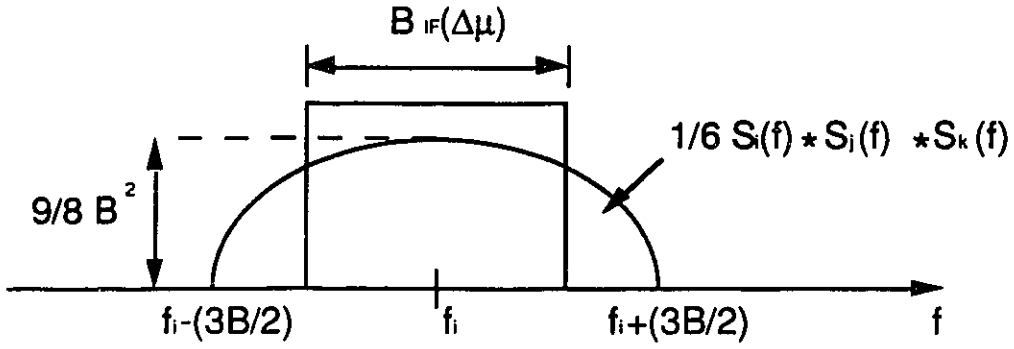

Figure A.2: Evaluation of the filtering coefficient for the IMD_3.

$$\begin{aligned}\int_{-\infty}^{+\infty} S_i(f) * S_j(f)|H_{BP}(f,\Delta\nu)|^2 df &= 2\int_{\frac{\Delta f}{2}-B}^{\frac{B_{IF}(\Delta\nu)}{2}} \left\{x + \left[B - \frac{\Delta f}{2}\right]\right\} dx \\ &= \frac{1}{4}\left[B_{IF}(\Delta\nu) + 2B - \Delta f\right]^2, \Delta f \leq B_{IF}(\Delta\nu) + 2B.\end{aligned} \tag{A.7}$$

Thus

$$h_2(\Delta\nu) = \begin{cases} \frac{1}{8}\left[\frac{B_{IF}(f}{B} + 2 - \frac{\Delta f}{B}\right]^2, & \Delta f \leq B_{IF}(\Delta\nu) + 2B; \\ 0, & \text{otherwise.} \end{cases} \tag{A.8}$$

An upper bound is used in [32] by letting $B = B_{IF}(\Delta\nu)$ in the expression of $S_i(f) * S_j(f)$. This assumption takes into account the broadening of the original signal spectrum due to the laser phase noise. The filtering coefficient for the IMD_2 then becomes

$$h_2(\Delta\nu) = \begin{cases} \frac{1}{8}\left[3 - \frac{\Delta f}{B_{IF}(\Delta\nu)}\right]^2, & \Delta f \leq 3B_{IF}(\Delta\nu); \\ 0, & \Delta f > 3B_{IF}(\Delta\nu). \end{cases} \tag{A.9}$$

The same procedure is followed in evaluating $h_3(\Delta\nu)$. From Fig. A.2, we see that

$$\begin{aligned} S_i(f) * S_j(f) * S_k(f) &= 6\int_{-B}^{f+\frac{B}{2}} [-|x| + B] dx \\ &= 3\left[-|f| + \frac{3}{2}B\right]^2. \end{aligned} \tag{A.10}$$

Thus

$$\int_{-\infty}^{+\infty} S_i(f) * S_j(f) * S_k(f) df = 2 \times 3 \int_0^{\frac{3B}{2}} \left[-|f| + \frac{3}{2}B \right]^2 df$$
$$= \frac{27}{4} B^3. \tag{A.11}$$

The numerator of (A.5) then becomes

$$\int_{-\infty}^{+\infty} S_i(f) * S_j(f) * S_k(f) |H_{BP}(f, \Delta\nu)|^2 df = 2 \times 3 \int_0^{\frac{B_{IF}(\Delta\nu)}{2}} \left[-|f| + \frac{3}{2}B \right]^2 df$$
$$= \frac{1}{4} \left[27B^3 - (3B - B_{IF}(\Delta\nu))^3 \right], \tag{A.12}$$

giving us finally that

$$h_3(\Delta\nu) = \frac{\frac{1}{4} \left[27B^3 - (3B - B_{IF}(\Delta\nu))^3 \right]}{\frac{27}{4} B^3}$$
$$= 1 - \left[1 - \frac{B_{IF}(\Delta\nu)}{3B} \right]^3. \tag{A.13}$$

Appendix B

Derivation of the IMD's Power for the OIM Scheme

The following is our derivation of the powers of the IMD_2 and IMD_3 in the case of OIM. The receiver photocurrent in the case of the OIM scheme is given by (3.31):

$$\begin{aligned} i_{IM}(t) &= 2R\sqrt{P_{LO}P_m}\left\{\sin\left(\frac{\alpha\pi}{4}\right) + m_{e_I}y(t)\cos\left(\frac{\alpha\pi}{4}\right) - \frac{1}{2!}[m_{e_I}y(t)]^2 \right. \\ &\left. \sin\left(\frac{\alpha\pi}{4}\right) + \frac{1}{3!}[m_{e_I}y(t)]^3\cos\left(\frac{\alpha\pi}{4}\right) + ...\right\}\cos[2\pi f_{IF}t + \theta(t)], \end{aligned} \tag{B.1}$$

where

$$y(t) = \sum_{j=1}^{N}\cos[2\pi f_j t + x_j(t)].$$

The first term in the right-hand side of (B.1) containing the information signal is

$$\begin{aligned} &2R\sqrt{P_{LO}P_m}m_{e_I}\cos\left(\frac{\alpha\pi}{4}\right)\left\{\sum_{j=1}^{N}\cos[2\pi f_j t + x_j(t)]\right\}\cos[2\pi f_{IF}t + \theta(t)] = \\ &R\sqrt{P_{LO}P_m}m_{e_I}\cos\left(\frac{\alpha\pi}{4}\right)\sum_j\{\cos[2\pi f_{IF}t + \theta(t) \pm 2\pi f_j t \pm x_j(t)]\}. \end{aligned} \tag{B.2}$$

The power of the signal in the kth subcarrier is then

$$< i_k^2 >= \frac{1}{2}R^2P_{LO}P_m\cos^2\left(\frac{\alpha\pi}{4}\right)m_{e_I}^2. \tag{B.3}$$

The second term can be rewritten as

$$-\frac{2R\sqrt{P_{LO}P_m}}{2!}\left(m_{e_I}\sum_j \cos[2\pi f_j t + x_j(t)]\right)^2 \sin\left(\frac{\alpha\pi}{4}\right)\cos[2\pi f_{IF}t + \theta(t)] =$$

$$-R\sqrt{P_{LO}P_m}m_{e_I}^2 \sin\left(\frac{\alpha\pi}{4}\right)\left\{\sum_j \cos^2[2\pi f_j t + x_j(t)] + \right.$$

$$\left. 2\sum_{i\neq j}\sum \cos[2\pi f_i t + x_i(t)]\cos[2\pi f_j t + x_j(t)]\right\}\cos[2\pi f_{IF}t + \theta(t)] =$$

$$-R\sqrt{P_{LO}P_m}m_{e_I}^2 \sin\left(\frac{\alpha\pi}{4}\right)\left\{\sum_j \frac{\cos[2(2\pi f_j t + x_j)] + 1}{2} + \right.$$

$$\left.\sum_{i\neq j}\sum \cos[2\pi(f_i \pm f_j) + (x_i \pm x_j)]\right\}\cos[2\pi f_{IF}t + \theta(t)]. \qquad \text{(B.4)}$$

The single summation in (B.4) contains the second-order harmonics and the double summation represents the second-order intermodulation distortion (IMD_2) terms of the type $f_i \pm f_j, i \neq j$. The second order harmonic in the kth subcarrier signal is thus

$$i_{2h} = -\frac{R\sqrt{P_{LO}P_m}}{4}m_{e_I}^2 \sin\left(\frac{\alpha\pi}{4}\right)\cos[2\pi f_{IF}t \pm 2(2\pi f_k t + x_k) + \theta(t)], \qquad \text{(B.5)}$$

and its mean-square value is

$$< i_{2h}^2 >= \frac{1}{32}R^2 P_{LO}P_m \sin^2\left(\frac{\alpha\pi}{4}\right)m_{e_I}^4 . \qquad \text{(B.6)}$$

From (B.4), the power of an IMD_2 term is four times that of a second-order harmonic; that is

$$< i_{2d}^2 >= \frac{1}{8}R^2 P_{LO}P_m \sin^2\left(\frac{\alpha\pi}{4}\right)m_{e_I}^4 . \qquad \text{(B.7)}$$

The total power of IMD_2 affecting the kth channel is then

$$< \sigma_{2d}^2 >= \frac{1}{8}R^2 P_{LO}P_m h_2(\Delta\nu)P_2(k)\sin^2\left(\frac{\alpha\pi}{4}\right)m_{e_I}^4 . \qquad \text{(B.8)}$$

The next term in the right-hand side of (B.1) can be expanded as follows:

$$\frac{2R\sqrt{P_{LO}P_m}}{3!}\left(m_{e_I}\sum_j \cos[2\pi f_j t + x_j(t)]\right)^3 \cos\left(\frac{\alpha\pi}{4}\right)\cos[2\pi f_{IF}t + \theta(t)] =$$

$$\frac{R\sqrt{P_{LO}P_m}}{3}m_{e_I}^3 \cos\left(\frac{\alpha\pi}{4}\right)\{\sum_j \cos^3[2\pi f_j t + x_j(t)] + 3\sum_{i\neq j}\sum \cos^2[2\pi f_i t + x_i]$$

$$\times \cos[2\pi f_j t + x_j(t)] + 6\sum\sum_{i\neq j\neq l}\sum \cos[2\pi f_i t + x_i(t)]\cos[2\pi f_j t + x_j(t)]$$

$$\times \cos[2\pi f_l t + x_l(t)]\}\cos[2\pi f_{IF}t + \theta(t)]. \qquad \text{(B.9)}$$

The single summation carries the third-order harmonics, while the triple summations represent the third-order intermodulation distortion (IMD_3). The third-order harmonic can be extracted from the single summation in (B.9) in the following way:

$$\frac{R\sqrt{P_{LO}P_m}}{3}m_{e_I}^3\cos\left(\frac{\alpha\pi}{4}\right)\left\{\sum_j\cos^3[2\pi f_j t+x_j(t)]\right\}\cos[2\pi f_{IF}t+\theta(t)]=$$
$$\frac{R\sqrt{P_{LO}P_m}}{3}m_{e_I}^3\cos\left(\frac{\alpha\pi}{4}\right)\left\{\frac{3}{4}\sum_j\cos[2\pi f_j t+x_j(t)]+\frac{1}{4}\sum_j\cos[3(2\pi f_j t+x_j(t))]\right\}$$
$$\times\cos[2\pi f_{IF}t+\theta(t)]. \tag{B.10}$$

The amplitude of the third-order harmonic in the kth subcarrier signal is then

$$i_{3h}=\frac{1}{24}R\sqrt{P_{LO}P_m}m_{e_I}^3\cos\left(\frac{\alpha\pi}{4}\right)\cos[2\pi f_{IF}t\pm 3(2\pi f_k t+x_k(t))+\theta(t)], \tag{B.11}$$

and its mean-square value is

$$<i_{3h}^2>=\frac{1}{2\times 24^2}R^2P_{LO}P_m\cos^2\left(\frac{\alpha\pi}{4}\right)m_{e_I}^6. \tag{B.12}$$

From (B.9), it can be seen that the amplitude of an IMD_3 term of the type $f_i\pm f_j\pm f_l, i\neq j\neq l$, is six (06) times that of a third-order harmonic. Thus

$$<i_{3d}^2>=\frac{1}{32}R^2P_{LO}P_m\cos^2\left(\frac{\alpha\pi}{4}\right)m_{e_I}^6. \tag{B.13}$$

Finally, the total power of IMD_3 falling in channel k is

$$<\sigma_{3d}^2>=\frac{1}{32}R^2P_{LO}P_m h_3(\Delta\nu)P_3(k)\cos^2\left(\frac{\alpha\pi}{4}\right)m_{e_I}^6. \tag{B.14}$$

References

[1] Richard A. Linke, "Optical heterodyne communications systems," *IEEE Commun. Mag.*, vol. 27, pp.36-41, Oct. 1989.

[2] L. G. Kazovsky, "Coherent optical receivers: performance analysis and laser linewidth requirements," *Optical Engineering*, vol. 25, pp. 575-579, Apr. 1986.

[3] M. Aissaoui and W. Steenaart, "Theoretical comparison of the effect of laser phase noise on coherent subcarrier-multiplexed photonic systems," *in Proc. Canadian Conference on Electrical and Computer Engineering, Toronto*, pp. WM2/24.1-24.4, Sept. 1992.

[4] R. Olshansky, V. A. Lanzisera, and P. M. Hill, "Subcarrier multiplexed lightwave systems for broadband distribution," *IEEE J. Lightwave Technol.*, vol. 7, pp. 1329-1341, Sept. 1989.

[5] E. Savov, *Multi-channel photonic networks*, Ph.D dissertation, Dept. of Electrical Eng., University of Ottawa, 1991.

[6] C. Desem, "Measurement of optical interference due to multiple optical carriers in subcarrier multiplexing," *IEEE Photonics Tech. Lett.*, vol. 3, pp. 387-389, Apr. 1991.

[7] T. H. Wood et al., "Broadband up-grade of a single-fiber fiber-in-the loop system using three levels of multiplexing," *Dig. OFC'92*, paper PD16, pp. 375-378, 1992.

[8] Q. Jiang and M. Kavehrad, "An optical multiaccess star network using subcarrier multiplexing," *IEEE Photonics Tech. Lett.*, vol. 4, pp. 1163-1165, Oct. 1992.

[9] L. G. Kazovsky, "Multichannel coherent optical communications systems," *IEEE J. Lightwave Technol.*, vol. LT-5, pp. 1095-1102, Aug. 1987.

[10] C. H. Henry, "Phase noise in semiconductor lasers," *IEEE J. Lightwave Technol.*, vol. LT-4, pp. 298-311, Mar. 1986.

[11] T. Okoshi and K. Kikuchi, *Coherent Optical Fiber Communications,* KTK Scientific Publishers, 1988.

[12] E. E. Hinkley and C. Freed, "Direct observation of the Lorentzian line shape as limited by quantum phase noise in a laser above threshold," *Phys. Rev. Lett.*, vol. 23, pp. 277-280, Aug. 1969.

[13] J. Salz, "Coherent lightwave communications," *Bell Sys. Tech. Jour.*, vol. 64, pp. 2153-2209, Dec. 1985.

[14] R. Gross and R. Olshansky, "Third-order intermodulation distortion in coherent subcarrier-multiplexed systems," *IEEE Photonics Tech. Lett.*, vol. 1, pp. 91-93, Apr. 1989.

[15] R. Gross, R. Olshansky, and P. Hill, "Five-channel coherent heterodyne subcarrier multiplexed system," *IEEE Photonics Tech. Lett.*, vol. 1, pp. 179-181, Jul. 1989.

[16] R. Gross, R. Olshansky, and P. Hill, "20 channel coherent FSK system using subcarrier multiplexing," *IEEE Photonics Tech. Lett.*, vol. 1, pp. 224-226, Aug. 1989.

[17] R. Gross, and R. Olshansky, "Multichannel coherent FSK experiments using subcarrier multiplexing techniques," *IEEE J. Lightwave Technol.*, vol. 8, pp. 406-415, Mar. 1990.

[18] L. G. Kazovsky, and D. A. Atlas, "Miniature NdYAG lasers: Noise and modulation characteristics," *IEEE J. Lightwave Technol.*, vol. 8, pp. 294-301, Mar. 1990.

[19] M. Okai et al., "Factors limiting the spectral linewidth of CPM-MQW-DFB lasers," *IEEE Photonics Tech. Lett.*, vol. 4, pp. 526-528, June 1992.

[20] G. L. Abbas, W. S. Chan, and T. K. Yee, "A dual-detector optical heterodyne receiver for local oscillator noise suppression," *IEEE J. Lightwave Technol.*, vol. LT-3, pp. 1110-1122, Oct. 1985.

[21] W. I. Way, "Subcarrier multiplexed lightwave system design considerations for subcarrier loop applications," *IEEE J. Lightwave Technol.*, vol. 7, pp. 1806-1818, Nov. 1989.

[22] S. B. Alexander, "Design of wide-band heterodyne balanced mixer receivers," *IEEE J. Lightwave Technol.*, vol. LT-5, pp. 523-537, Apr. 1987.

[23] R. Gross, P. Meissner, and E. Patzak, "Theoretical investigation of local oscillator intensity noise in optical heterodyne systems," *IEEE J. Lightwave Technol.*, vol. 6, pp. 521-530, Apr. 1988.

[24] R. M. Gagliardi and S. Karp, *Optical Communications*, John Wiley & Sons, 1976.

[25] Y. Yamamoto and T. Kimura, "Coherent optical fiber transmission systems," *IEEE J. Quantom Electron.*, vol. QE-17, pp. 919-934, Jun. 1981.

[26] T. Okoshi, "Heterodyne and coherent optical fiber communications: recent progress," *IEEE Trans. Microwave Theory Techniques* , vol. MTT-30, pp. 1138-1149, Aug. 1982.

[27] T. Okoshi, "Polarization-state control schemes for heterodyne or homodyne optical fiber communications," *IEEE J. Lightwave Technol.*, vol. LT-3, pp. 1232-1237, Dec. 1985.

[28] G. R. Walker and N. G. Walker, "Rugged all-fiber endless polarization controller," *Electron. Lett.*, vol. 24, pp. 1353-1354, Oct. 1988.

[29] M. Kavehrad and B. Glance, "A polarization-insensitive frequency shift keying optical heterodyne receiver using discriminator demodulation," *IEEE J. Lightwave Technol.*, vol. 6, pp. 1386-1392, Sept. 1988.

[30] L. G. Kazovsky, "Phase- and polarization-diversity coherent optical techniques," *IEEE J. Lightwave Technol.*, vol. 7, pp. 279-292, Feb. 1989.

[31] E. Savov, W. Steenaart, and M. Kavehrad, "Theoretical comparison of modulation methods for coherent subcarrier-multiplexed photonic systems," *in Proc. MILCOM'90, Monterey, CA.*, pp. 574-578, Sept. 1990.

[32] Yang-Han Lee, J. Wu, and Hen-Wai Tsao, "The impact of laser phase noise on the coherent subcarrier multiplexing system," *IEEE J. Lightwave Technol.*, vol. 9, pp. 347-355, March 1991.

[33] F. C. Allard, *Fiber Optics Handbook for Engineers and Scientists,* ch. 7, McGraw-Hill Publishing Company, 1990.

[34] M. Ross, *Laser Receivers,* John Wiley & Sons, 1966.

[35] A. Yariv, *Optical Electronics,* ch. 9, Holt, Rinehart and Winston, 1985.

[36] R. C. Alferness, "Waveguide electrooptic modulators," *IEEE Trans. Microwave Theory Techniques,* vol. MTT-30, pp. 1121-1137, Aug. 1982.

[37] L. G. Kazovsky and G. Jacobsen, "Multichannel CPFSK coherent optical communications systems," *IEEE J. Lightwave Technol.*, vol. 7, pp. 972-982, Jun. 1989.

[38] K. Iwashita and T. Matsumoto, "Modulation and detection characteristics of optical continuous phase FSK transmission system," *IEEE J. Lightwave Technol.*, vol. LT-5, pp. 452-460, Apr. 1987.

[39] T. E. Darcie, "Subcarrier multiplexing for multiple-access lightwave networks," *IEEE J. Lightwave Technol.*, vol. LT-5, pp. 1103-1110, Aug. 1987.

[40] L. G. Kazovsky and J. L. Gimlett, "Sensitivity penalty in multichannel coherent optical communications," *IEEE J. Lightwave Technol.*, vol. 6, pp. 1353-1365, Sept. 1988.

[41] R. Wyatt and W. J. Devlin, "10 KHz linewidth 1.5μm InGasP external cavity laser with 55 nm tuning range," *Electron. Lett.*, vol. 19, pp. 110-112, Feb. 1983.

[42] J. M. Wozencraft and I. M. Jacobs, *Principles of Communication Engineering,* John Wiley & Sons, 1965.

[43] M. Azizoglu, *Phase noise in coherent optical communications,* Ph.D dissertation, Laboratory for Information and Decision Systems, MIT, Cambridge, MA, 1991.

[44] L. G. Kazovsky, "Balanced phase-locked loops for optical homodyne receivers: performance analysis, design considerations and linewidth requirements," *IEEE J. Lightwave Technol.,* vol. LT-4, pp. 182-195, Feb. 1986.

[45] A. W. Davis et al., "Phase diversity techniques for coherent optical receivers," *IEEE J. Lightwave Technol.,* vol. LT-5, pp. 561-572, Apr. 1987.

[46] I. Garrett et al., "Weakly coherent optical systems using lasers with significant phase noise," *IEEE J. Lightwave Technol.,* vol.6, pp. 1520-1526, Oct. 1988.

[47] L. G. Kazovsky et al., "Wide-linewidth phase diversity homodyne receivers," *IEEE J. Lightwave Technol.,* vol.6, pp. 1527-1536, Oct. 1988.

[48] P. A. Humblet and M. Azizoglu, "On the bit error rate of lightwave systems with optical amplifiers," *IEEE J. Lightwave Technol.,* vol. 9, pp. 1576-1582, Nov. 1991.

[49] Y. H. Cheng and T. Okoshi, "Phase-noise-cancelling dual-frequency heterodyne optical fibre communication system," *Electron. Lett.,* vol. 25, pp. 835-836, June 1989.

[50] K. Tamura, S. B. Alexander, and V. W. S. Chan, "Phase-noise -canceled differential-phase-shift-keying PNC-DPSK modulation for coherent optical communication systems," in *Optical Fiber Communications Conf.,* Paper WG2, Jan. 1988.

[51] K. Tamura et al., "Phase-noise canceled differential-phase -shift-keying PNC-DPSK modulation for coherent optical communication systems," *IEEE J. Lightwave Technol.,* vol. 8, pp. 190-201, Feb. 1990.

[52] Y. Imai, K. Iizuka, and R. T. B. James, "Phase-noise free coherent optical communication system utilizing differential polarization shift keying (DPolSK)," *IEEE J. Lightwave Technol.*, vol. 8, pp. 691-697, May 1990.

[53] R. Gross, R. Olshansky, and M. Schmidt, "Coherent FM-SCM system using DFB lasers and a phase noise cancellation circuit," *IEEE Photonics Tech. Lett.*, vol. 2, pp. 66-68, Jan. 1990.

[54] R. Gross and R. Olshansky, "Second-order IMD cancellation receiver for wideband coherent SCM systems," *IEEE Photonics Tech. Lett.*, vol. 3, pp. 847-849, Sept. 1991.

[55] R. S. Bondurant et al., "Frequency-noise cancellation in semiconductor lasers by nonlinear heterodyne detection," *Optics Lett.*, vol. 11, pp. 791-793, Dec. 1986.

[56] X. Zhang and P. Jiang, "Phase-noise-insensitive coherent optical heterodyne CPFSK receiver with limiter-discriminator detector," *IEEE Photonics Tech. Lett.*, vol. 3, pp. 543-544, June. 1991.